Molecular Biology of the Cell
Vol. 11, 287–304, January 2000

Selective Alterations in Biosynthetic and Endocytic Protein Traffic in Madin-Darby Canine Kidney Epithelial Cells Expressing Mutants of the Small GTPase Rac1

Tzuu-Shuh Jou,*† Som-Ming Leung,‡ Linette M. Fung,* Wily G. Ruiz,‡ W. James Nelson,* and Gerard Apodaca‡§

*Department of Molecular and Cellular Physiology, Stanford University School of Medicine, Stanford, California 94305-5345; and ‡Renal-Electrolyte Division of the Department of Medicine and Laboratory of Epithelial Biology, University of Pittsburgh, Pittsburgh, Pennsylvania 15261

Submitted July 28, 1999; Revised September 29, 1999; Accepted October 15, 1999
Monitoring Editor: David Drubin

Madin-Darby canine kidney (MDCK) cells expressing constitutively active Rac1 (Rac1V12) accumulate a large central aggregate of membranes beneath the apical membrane that contains filamentous actin, Rac1V12, rab11, and the resident apical membrane protein GP-135. To examine the roles of Rac1 in membrane traffic and the formation of this aggregate, we analyzed endocytic and biosynthetic trafficking pathways in MDCK cells expressing Rac1V12 and dominant inactive Rac1 (Rac1N17). Rac1V12 expression decreased the rates of apical and basolateral endocytosis, whereas Rac1N17 expression increased those rates from both membrane domains. Basolateral-to-apical transcytosis of immunoglobulin A (IgA) (a ligand for the polymeric immunoglobulin receptor [pIgR]), apical recycling of pIgR-IgA, and accumulation of newly synthesized GP-135 at the apical plasma membrane were all decreased in cells expressing Rac1V12. These effects of Rac1V12 on trafficking pathways to the apical membrane were the result of the delivery and trapping of these proteins in the central aggregate. In contrast to abnormalities in apical trafficking events, basolateral recycling of transferrin, degradation of EGF internalized from the basolateral membrane, and delivery of newly synthesized pIgR from the Golgi to the basolateral membrane were all relatively unaffected by Rac1V12 expression. Rac1N17 expression had little or no effect on these postendocytic or biosynthetic trafficking pathways. These results show that in polarized MDCK cells activated Rac1 may regulate the rate of endocytosis from both membrane domains and that expression of dominant active Rac1V12 specifically alters postendocytic and biosynthetic membrane traffic directed to the apical, but not the basolateral, membrane.

INTRODUCTION

The compartmentalized nature of the eukaryotic cell requires a highly regulated protein trafficking system to establish and maintain membrane, organellar, and cellular identity (Mostov and Cardone, 1995). As a result, the quality and quantity of biosynthetic and endocytic traffic must be capable of changing in response to extracellular signals. The Rho family of small GTPases represents an important class of molecules that can adjust cellular functions in response to a variety of extracellular signals (Van Aelst and D'Souza-Schorey, 1997). This family currently comprises at least seven members and their isoforms (Mackay and Hall, 1998): Rho (A and B isoforms), Rac (1 and 2 isoforms), Cdc42 (Cdc42Hs and G25K isoforms), RhoD, RhoG, RhoE, and TC10. Initially, Rho family members were shown to regulate the formation of specialized actin structures in the cell: RhoA controls the formation of stress fibers and focal adhesion (Ridley and Hall, 1992), Rac1 directs lamellipodia formation (Ridley *et al.*, 1992), and Cdc42 modulates the assembly of filopodia (Kozma *et al.*, 1995). In addition, it is now clear that the Rho family of GTPases controls diverse cellular events, including transcription, cell growth, development, and membrane traffic (Vojtek and Cooper, 1995; Van Aelst and D'Souza-Schorey, 1997; Hall, 1998).

Multiple membrane trafficking events appear to be modulated by Rho family members, including phagocytosis of *Shi-*

† Present address: Graduate Institute of Clinical Medicine, College of Medicine, National Taiwan University, Taipei, 100 Taiwan.
§ Corresponding author. E-mail address: gla6@pitt.edu.
Abbreviations used: ARE, apical recycling endosome; DAB, diaminobenzidine; DC, doxycycline; ER, endoplasmic reticulum; IgA, immunoglobulin A; MDCK, Madin-Darby canine kidney; pIgR, polymeric immunoglobulin receptor; PI-3-K, phosphatidylinositol-3-kinase; Tf, transferrin; TGN, *trans*-Golgi network.

gella by RhoA (Adam *et al.*, 1996; Watarai *et al.*, 1997) and of *Salmonella* by Cdc42 (Chen *et al.*, 1996), pinocytosis by Rac1 (Schmalzing *et al.*, 1995), and receptor-mediated endocytosis by RhoA and Rac1 (Lamaze *et al.*, 1996; Leung *et al.*, 1999). RhoA may also regulate transcytosis and recycling in polarized Madin-Darby canine kidney (MDCK) cells (Leung *et al.*, 1999). RhoB is localized to early endosomes and synaptic microvesicles (Adamson *et al.*, 1992; Cussac *et al.*, 1996), and RhoD is found on early endosomes and the plasma membrane (Murphy *et al.*, 1996). Expression of constitutively active RhoD decreases endosome motility (Murphy *et al.*, 1996). Rho family members also regulate secretion. In mast cells, RhoA, Rac1, and Cdc42 stimulate exocytosis of secretory granules, whereas C-3 transferase and dominant inactive RhoA and Rac1 inhibit guanosine 5′-*O*-(3-thiotriphosphate)-stimulated secretion (Norman *et al.*, 1994, 1996; Price *et al.*, 1995; Mariot *et al.*, 1996; O'Sullivan *et al.*, 1996; Brown *et al.*, 1998). New evidence indicates that Cdc42 may be important in regulating the delivery of newly synthesized proteins to the basolateral domain of polarized MDCK epithelial cells (Kroschewski *et al.*, 1999).

Recently, we analyzed the effect of the expression of RhoA and Rac1 mutants on the development of polarity of MDCK cells (Jou and Nelson, 1998). The establishment and maintenance of epithelial cell polarity require cell-cell and cell-substratum interactions, remodeling of the cytoskeleton, and the development of directionality in membrane trafficking pathways to the apical and basolateral membrane domains (Drubin and Nelson, 1996). During the development of cell polarity, Rac1V12 expression caused the redistribution of GP-135, an apical membrane protein, to a large central aggregate of membranes located beneath the apical membrane domain (Jou and Nelson, 1998). This aggregate contained Rac1V12 and filamentous actin. Significantly, we also detected the small GTPase rab11 in the aggregate; rab11 is normally found on the *trans*-Golgi network (TGN) and recycling endosomes and is known to regulate endosome function (Urbé *et al.*, 1993; Ullrich *et al.*, 1996; Green *et al.*, 1997; Ren *et al.*, 1998; Casanova *et al.*, 1999). The presence of rab11 on this central aggregate indicated that the aggregate may be an endosomal compartment and, therefore, that Rac1 might have a previously unappreciated role in regulating endocytic membrane traffic. The goals of our current analysis were severalfold: to determine the origin of the large central aggregate in Rac1V12-expressing cells; to analyze the effects of Rac1V12 and dominant inactive Rac1 (Rac1N17) expression on biosynthetic traffic in MDCK cells; and to determine if constitutively active or dominant inactive Rac1 regulates endocytic traffic.

MATERIALS AND METHODS

Cell Lines and Cell Culture

MDCK cells (T23 clone) expressing dominant active myc-tagged Rac1V12 or dominant negative myc-tagged Rac1N17 under the control of a tetracycline-repressible transactivator have been described previously (Jou and Nelson, 1998). The cells were routinely cultured in DMEM containing 10% (vol/vol) FBS (DMEM/FBS), 100 U/ml penicillin/100 μg/ml streptomycin, and 20 ng/ml doxycycline (DC) (Sigma Chemical, St. Louis, MO) at 37°C in a humidified atmosphere containing 5% CO_2. The DC stock solution (20 μg/ml in 95% ethanol) was stored at −20°C and was diluted 1:1000 just before use. Expression of Rac1V12 or Rac1N17 was induced by plating cells in 15-cm dishes at low density into DMEM/FBS medium lacking DC and incubating them for 16–20 h (Rac1N17) or 36 h (Rac1V12) at 37°C. At the end of this incubation period, the cells had reached ~30% confluence. Cells treated in an identical manner, but in the presence of 20 ng/ml DC, served as controls. The cells were trypsinized and washed with culture medium containing 5 μM calcium chloride, and 1×10^6 cells (resuspended in 0.5 ml of 5 μM calcium chloride) were added to the apical chamber of rat-tail, collagen-coated, 12-mm-diameter Transwells (Corning-Costar, Cambridge, MA) in 5 μM calcium chloride (with or without 20 ng/ml DC). Cells were incubated in 5 μM calcium chloride for 3–4 h, rinsed twice with Dulbecco's PBS lacking calcium and magnesium, and then incubated in DMEM/FBS containing normal amounts of calcium chloride (1.8 mM) for 18–48 h (with or without 20 ng/ml DC).

Antibodies, Proteins, and Other Markers

The following reagents were used: mouse anti-myc hybridoma 9E10 (Dr. Gordan Cann, Stanford University, Stanford, CA); mouse anti-GP-135 hybridoma 3F2/D8 (Dr. G. Ojakian, State University of New York, Brooklyn, NY); rabbit polyclonal anti-mp30/BAP31, an endoplasmic reticulum (ER) resident protein (Dr. P. Walter, University of California, San Francisco, CA); rabbit polyclonal anti-mouse furin, a TGN resident protein (Alexis Biochemicals, San Diego, CA); mouse monoclonal anti-giantin, a Golgi resident protein (Dr. A. Lindstedt, Carnegie Mellon University, Pittsburgh, PA); mouse monoclonal anti-lysosomal membrane protein hybridoma Ac17 (Dr. E. Rodriguez-Boulan, Cornell University, New York, NY); rat anti-ZO-1 hybridoma R40.76 (Dr. D.A. Goodenough, Harvard University, Cambridge, MA); mouse anti-Rac1 (Transduction Laboratories, Lexington, KY); affinity-purified rabbit polyclonal anti-rab11 antibody (Zymed Laboratories, South San Francisco, CA); affinity-purified rabbit polyclonal anti-human immunoglobulin A (IgA) (Jackson Immunoresearch Laboratories, West Grove, PA); polyclonal mouse anti-canine transferrin (Tf) prepared from mice sensitized to canine Tf with the use of standard immunological protocols; affinity-purified and minimal cross-reacting fluorescein-, Texas red–, and Cy5-conjugated secondary antibodies (Jackson Immunoresearch Laboratories); human polymeric IgA (Dr. K. Mostov, University of California, San Francisco, CA); rhodamine phalloidin (Molecular Probes, Eugene, OR); and Fab fragments of affinity-purified polyclonal sheep anti-secretory component conjugated to HRP (Dr. K. Mostov).

Western Blot Analysis

Filter-grown cells were lysed in 0.2 ml of 0.5% SDS lysis buffer (100 mM triethanolamine, pH 8.6, 5 mM EDTA, 0.5% SDS), boiled for 3 min, and then vortex shaken for 15 min at 4°C to shear the DNA. The samples were centrifuged at 13,000 × *g*, and 10 μl of the sample was mixed with an equal volume of 2× Laemmli sample buffer containing 100 mM DTT, heated to 100°C for 3 min, and then resolved by SDS-PAGE in 15% (wt/vol) polyacrylamide gels. The proteins were transferred to Immobilon-P membranes (Millipore, Bedford, MA) for 75 min at 375 mA, and the membrane was blocked for 30 min in 10% (wt/vol) BSA dissolved in Dulbecco's PBS. Blotted proteins were reacted with primary antibodies (diluted in PBS containing 1% dehydrated nonfat milk) for 2 h at room temperature with rotation. The membrane was then washed with Tris-buffered saline–Tween (2.68 mM KCl, 0.5 M NaCl, 25 mM Tris-HCl, pH 8.0, 0.05% [vol/vol] Tween-20) three times for 15 min each and then incubated in the appropriate secondary antibody conjugated to HRP diluted 1:25,000 in PBS containing 1% dehydrated nonfat milk for 1 h with rotation. The membrane was washed three times for 15 min each with Tris-buffered saline–Tween, incubated for 1 min in Super Signal (Pierce, Rockford, IL), and exposed to XAR-5 film (Kodak, Rochester, NY). Relative intensities of the protein bands were quantified by densitometry.

Immunofluorescence Labeling and Scanning Laser Confocal Microscopy

Cells were fixed and processed for immunofluorescence with the use of either 3.7% paraformaldehyde (Jou and Nelson, 1998) or a pH shift protocol (Apodaca *et al.*, 1994). Photomicrographs were obtained by photographing epifluorescence images acquired with an Axioplan fluorescence microscope (Carl Zeiss, Thornwood, NY) fitted with 40× or 63× oil immersion lenses or by capturing digital images with a TCS confocal microscope equipped with krypton, argon, and helium-neon lasers (Leica, Deerfield, IL). Images obtained with the TCS confocal microscope were acquired with the use of a 100× plan-apochromat objective (numerical aperture 1.4) and the appropriate filter combination. Settings were as follows: photomultipliers were set to 600–800 mV, 1.5-μm pinhole, zoom = 3.0, Kalman filter (n = 4). The images (1024 × 1024 pixels) were saved in tag-information-file-format, and the contrast levels of the images were adjusted in the Photoshop program (Adobe, Mountain View, CA) on a Power PC G-3 Macintosh computer (Apple, Cupertino, CA). The contrast-corrected images were imported into Freehand (Macromedia, San Francisco, CA) and printed from a Kodak 8650PS dye sublimation printer.

Electron Microscopic Analysis of Cells Expressing Rac1V12

After internalization of Fab-HRP, cells were washed three times quickly with MEM/BSA (MEM containing 0.25 g/l $NaHCO_3$, 0.6% BSA, and 20 mM HEPES, pH 7.4) and one time with ice-cold PBS^+ (PBS containing 0.5 mM $MgCl_2$, 0.9 mM $CaCl_2$). The cells were immediately fixed by adding ice-cold 0.5% (vol/vol) glutaraldehyde in 200 mM Na cacodylate, pH 7.4, 1 mM $CaCl_2$, 0.5 mM $MgCl_2$ and incubating the cells for 30 min at room temperature. The cells were rinsed three times with 200 mM Na cacodylate buffer, pH 7.4, and 0.1% (wt/vol) diaminobenzidine (DAB; dissolved in 200 mM cacodylate buffer) was added for 2 min at room temperature. The DAB solution was aspirated and replaced with fresh DAB solution containing 0.01% (vol/vol) H_2O_2 and incubated for 30 min at room temperature in the dark. Samples were rinsed with 200 mM Na cacodylate, pH 7.4, and osmicated with 1% (wt/vol) OsO_4, 200 mM Na cacodylate, pH 7.4, 1% (wt/vol) $K_4Fe(CN)_6$ for 90 min at 4°C. After several rinses with H_2O, samples were *en bloc* stained overnight with 0.5% (wt/vol) uranyl acetate in H_2O. Filters were dehydrated in a graded series of ethanol, embedded in the epoxy resin LX-112 (Ladd, Burlington, VT), and sectioned with a diamond knife (Diatome, Fort Washington, PA). Sections, pale gold in color, were mounted on butvar-coated nickel grids and viewed at 80 kV in a JEOL (Japan) 100 CX electron microscope without further contrasting.

Endocytosis of [^{125}I]IgA

Endocytosis of [^{125}I]IgA was measured as described (Breitfeld *et al.*, 1990). [^{125}I]IgA was iodinated with the use of the ICl method to a specific activity of 1.0–2.0 × 10^7 cpm/μg (Breitfeld *et al.*, 1989a). Cells were rapidly cooled and washed three times with ice-cold MEM/BSA. [^{125}I]IgA diluted in MEM/BSA was bound to either the apical or the basolateral surface of the cells for 60–90 min at 4°C. Cells were washed three times quickly and then three times for 10 min with MEM/BSA (the final washes were performed by incubating the cells on a rotator). Cells were then either left on ice or warmed to 37°C for periods up to 10 min. At the conclusion of the experiment, [^{125}I]IgA was stripped from the cell surface by incubating the cells for 60 min at 4°C with 100 μg/ml trypsin followed by an acid treatment with 750 mM glycine, pH 2.5, diluted 1:5 with PBS^+. The Transwells were rinsed with PBS^+, and the filters were cut out of their holders. Total [^{125}I]IgA initially bound to the cells included ligand dissociated from the cell surface, ligand stripped from the cell surface with trypsin and acid, and cell-associated ligand not sensitive to trypsin and acid stripping (endocytosed); it was quantified with a gamma counter.

Measurement of Paracellular Diffusion of [^{125}I]IgA and [^{125}I]Tf

Filter-grown cells were washed three times with MEM/BSA and [^{125}I]IgA or [^{125}I]Tf, diluted in 0.5 ml of MEM/BSA containing a 100-fold excess of unlabeled IgA or Tf, and added to the apical chamber of the Transwell. Cold competing ligand was added to prevent receptor-mediated internalization and apical-to-basolateral transcytosis. MEM/BSA (0.5 ml) was placed in the basolateral chamber. At the designated times, the basolateral MEM/BSA (0.5 ml) was collected and replaced with fresh MEM/BSA. After the final time point, filters were washed twice with ice-cold PBS and cut out of the insert, and the amount of [^{125}I]IgA or [^{125}I]Tf that remained in the apical medium, that had diffused into the basolateral chamber, or that remained cell associated was quantified with a gamma counter. The results are expressed as percentages of [^{125}I]IgA or [^{125}I]Tf initially added to the apical chamber that was released basolaterally.

Analysis of [^{125}I]IgA Postendocytic Fate

The postendocytic fate of a preinternalized cohort of [^{125}I]IgA (at 5–10 μg/ml) was analyzed as described (Breitfeld *et al.*, 1989b). In brief, [^{125}I]IgA, diluted in MEM/BSA, was internalized from either the apical or the basolateral pole of the cells for 10 min at 37°C. Subsequently, the cell surface from which ligand was internalized was washed rapidly three times with MEM/BSA, and the apical and basolateral media were aspirated and replaced with fresh MEM/BSA. The cells were then incubated for 3 min at 37°C. This total wash procedure took 5 min at 37°C. Fresh MEM/BSA was added to the cells, which were chased for up to 2 h at 37°C. At the designated times, the apical and basolateral MEM/BSA media (0.5 ml) were collected and replaced with fresh MEM/BSA. After the final time point, filters were cut out of the insert and the amount of [^{125}I]IgA was quantified with a gamma counter. The MEM/BSA samples were precipitated with 10% trichloroacetic acid for 30 min on ice and then centrifuged in a microfuge for 15 min at 4°C. The amount of [^{125}I]IgA in the trichloroacetic acid–soluble (degraded) and trichloroacetic acid–insoluble (intact) fractions was quantified with a gamma counter. In the original description of the assay, values for untransfected MDCK cells were subtracted from those for MDCK cells expressing the polymeric immunoglobulin receptor (pIgR) as a correction for fluid-phase internalization (Breitfeld *et al.*, 1989b). Because we did not have MDCK cells expressing the Rac1 constructs but not pIgR, we did not feel that an original clone of MDCK cells was a suitable control. Instead, in preliminary experiments, we performed assays in the presence of a 100-fold excess of cold competing IgA. We found that the amount of fluid-phase internalization was <5% of the signal observed in pIgR-expressing cells. Because this correction for fluid-phase internalization did not alter the results significantly, this step was omitted in subsequent experiments.

Analysis of [^{125}I]Tf Recycling

Iron-saturated Tf was iodinated to a specific activity of 5.0–9.0 × 10^6 cpm/μg with the use of ICl as described (Apodaca *et al.*, 1994). The cells were washed with warm (37°C) MEM/BSA three times, and unlabeled Tf was allowed to dissociate from the cell surface and filter for 60 min in MEM/BSA. [^{125}I]Tf (5 μg/ml) was internalized from the basolateral surface of the cells for 45 min at 37°C in a humid chamber. The cells were washed three times for 5 min each with ice-cold MEM/BSA and then warmed to 37°C for 2.5 min to allow for receptor internalization, as described previously (Apodaca *et al.*, 1994). The medium was aspirated, fresh medium was added, and the postendocytic fate of [^{125}I]Tf was assessed as described above. [^{125}I]Tf uptake was inhibited >95% when the

radioactive ligand was internalized in the presence of a 100-fold excess of cold ligand.

Analysis of [^{125}I]EGF Degradation

[^{125}I]EGF (150–200 μCi/μg) was purchased from New England Nuclear Life Science Products (Boston, MA) and used at a final concentration of 40 ng/ml. The cells were washed with warm (37°C) MEM/BSA three times, and [^{125}I]EGF was internalized from the basolateral surface of the cells for 10 min at 37°C. The cells were washed rapidly three times with MEM/BSA, the apical and basolateral media were aspirated and replaced with fresh MEM/BSA, and the cells were then incubated for 3 min at 37°C. The media were aspirated, fresh media were added, and the postendocytic fates of [^{125}I]EGF and trichloroacetic acid precipitations of media samples were assessed as described above.

Treatment with Nocodazole or CD

When specified, cells were pretreated for 30–60 min at 4°C with 33 μM nocodazole, and the drug was included in all subsequent incubations steps. In some experiments, 25 μg/ml CD was included in the MEM/BSA. Both nocodazole and CD were prepared in DMSO as 1000-fold concentrated stocks and stored at −20°C.

Cell-Surface Delivery Assays

Basolateral delivery of the pIgR was assessed as described previously (Aroeti and Mostov, 1994). Delivery of newly synthesized GP-135 from the Golgi to the apical membrane was determined as described previously (Grindstaff *et al.*, 1998a).

RESULTS

Induction of Rac1 Overexpression in Polarized MDCK Cells

Previously, we established the T23 clone of MDCK cells that stably expresses the tetracycline transactivator (Barth *et al.*, 1997). Subsequently, we generated clones of T23 cells in which expression of either NH_2-terminal myc-tagged dominant active Rac1V12 or dominant inactive Rac1N17 was controlled by a tetracycline transactivator (Jou and Nelson, 1998). The T23 clone of MDCK cells also expresses pIgR.

Expression levels of Rac1V12 or Rac1N17 were controlled by the addition of DC to the growth medium. In the presence of 20 ng/ml DC, neither Western blotting (Figure 1) nor immunofluorescence microscopy (Figure 2) detected expression of either Rac1V12 or Rac1N17. However, in the absence of DC, Western blotting showed that the amount of Rac1V12 expressed in cells 18 h after plating on Transwells was ~80% of the level of endogenous Rac1, and after 36–48 h it was ~50% (Figure 1). By 72 h, the amount of Rac1V12 expressed was undetectable (Leung, unpublished results). This latter observation is consistent with our previous observation that the levels of these exogenous proteins are down-regulated over time (Jou and Nelson, 1998). In the biochemical experiments described below, we used cells 18–48 h after plating and obtained similar results; at these times, polarized trafficking of proteins to apical and basolateral membrane domains occurs (Grindstaff *et al.*, 1998b). The level of Rac1N17 expression was ~500% of that of endogenous Rac1 and remained at that level >48 h after plating of cells on Transwells (Figure 1).

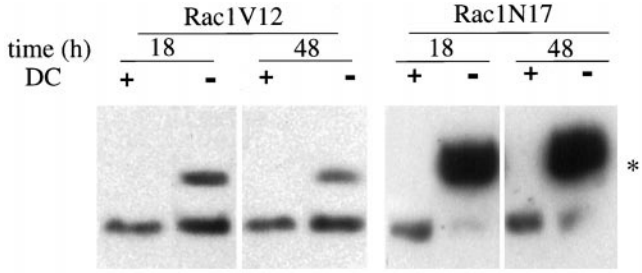

Figure 1. Inducible expression of myc-tagged Rac1V12 and Rac1N17 in polarized MDCK cells. Rac1V12 or Rac1N17 cells were plated at low density in medium lacking DC (−) or containing DC (+), incubated for 16–20 h (Rac1N17) or 36 h (Rac1V12), and then plated on Transwell filter supports (with or without DC). At the designated times, the filter-grown cells were solubilized in SDS lysis buffer and processed for Western blotting with an anti-Rac1 mAb to detect induction of the myc-tagged mutant proteins as well as endogenous Rac1. (*) The addition of the myc tag to Rac1V12 and Rac1N17 causes these proteins to migrate slower than endogenous Rac1.

The Central Aggregate Observed in Rac1V12-expressing MDCK Cells Primarily Contains Markers of the Early Endosomal System

To determine the origin of the membranous aggregate, we examined whether marker proteins of the ER, Golgi, TGN, early endosome, or late endosome/lysosome colocalized with Rac1V12 in this structure. The presence of any of these marker proteins in the aggregate might identify which membrane trafficking pathway(s) was affected by Rac1V12 expression.

Because the central aggregate contained rab11, a marker of endosomal recycling compartments (Ullrich *et al.*, 1996; Green *et al.*, 1997; Ren *et al.*, 1998; Casanova *et al.*, 1999), we first examined the distribution of several marker proteins of the endocytic pathway in Rac1V12- and Rac1N17-expressing cells, including (a) basolaterally internalized IgA (a pIgR ligand), which is transported to the apical cell surface via a series of endosomal compartments, including basolateral early endosomes, the common endosome (Odorizzi *et al.*, 1996), and the apical recycling endosome (ARE) (Apodaca *et al.*, 1994); (b) basolaterally internalized Tf, which recycles back to the basolateral membrane (Fuller and Simons, 1986) from the basolateral early endosomes and the common endosome (Sheff *et al.*, 1999); (c) apically internalized IgA, which primarily recycles back to the apical membrane (Apodaca *et al.*, 1994); and (d) the Ac17 antigen, which recognizes a lysosomal membrane protein that is found primarily in late endosomes, lysosomes, and basolateral early endosomes (Nabi *et al.*, 1991).

To determine if IgA is delivered to the central Rac1V12 aggregate, we followed the fate of IgA internalized from the basolateral membrane of control cells and cells expressing Rac1V12. In control cells grown in the presence of DC, IgA was rapidly delivered to the apical pole of the cell, where it was found in punctate membrane structures that lie above the nucleus and at the level of the tight junction (Figure 2, A and B). These structures have previously been characterized as elements of the common endosome/ARE (Apodaca *et al.*, 1994; Barroso and Sztul, 1994; Odorizzi *et al.*, 1996). As expected, we did not detect myc-tagged Rac1V12 in these

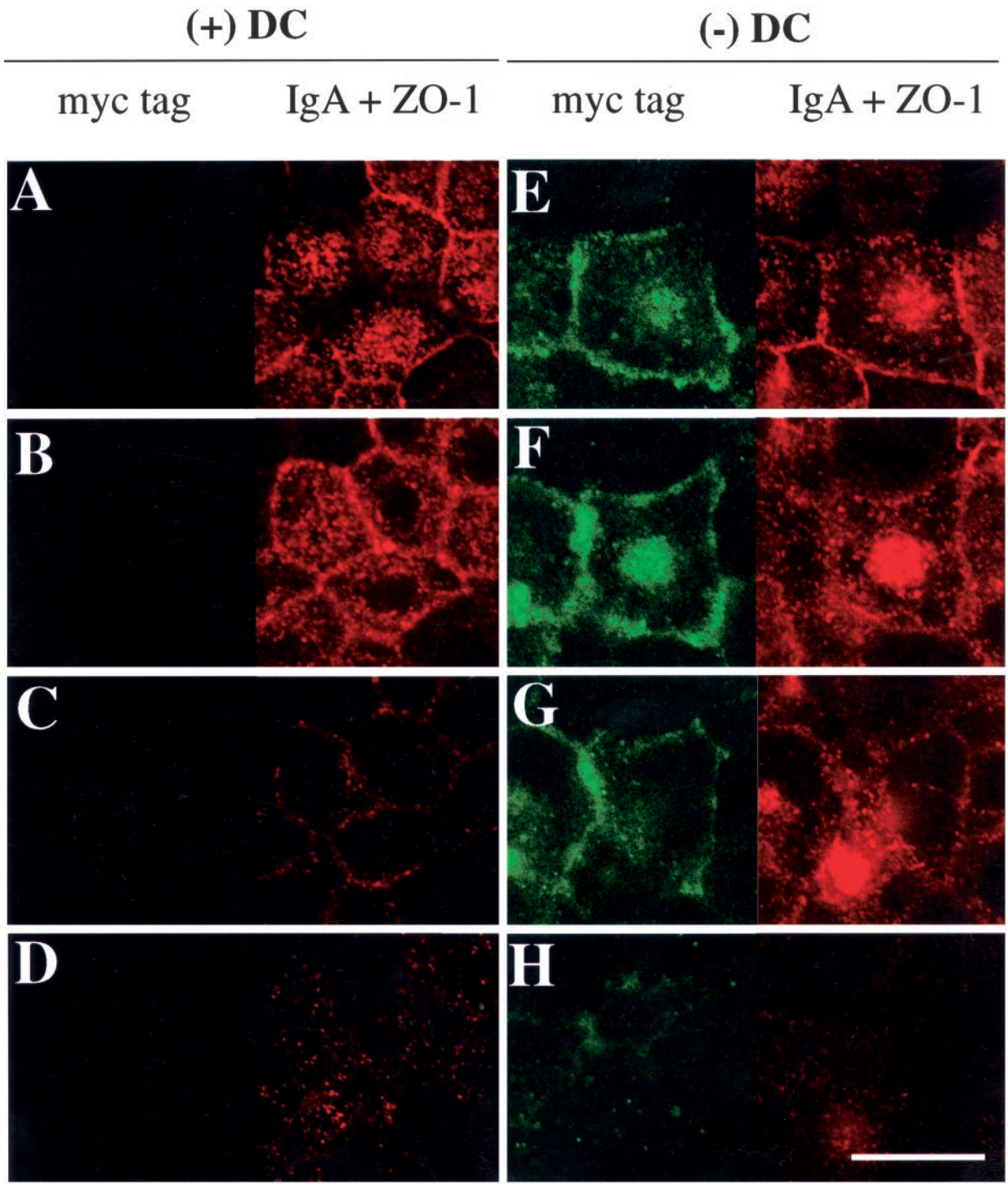

Figure 2. Distribution of basolaterally internalized IgA and myc-tagged Rac1V12 in cells grown in the absence (−) or presence (+) of DC. IgA was internalized from the basolateral surface for 10 min at 37°C in Rac1V12 cells grown in the presence (A–D) or absence (E–H) of DC and then washed and chased for 5 min at 37°C. Cells were fixed with paraformaldehyde and stained with the appropriate antibodies, and FITC and Cy5 emissions (which are displayed in the left and right halves of each panel, respectively) were captured with the use of a scanning laser confocal microscope. Shown are optical sections from the base of the cells (D and H), along the lateral surface of the cells (C and G), above the nucleus (B and F), and at or above the level of the tight junctions (A and E). Note that there are at least 2–3 μm between each optical section. The tight junctions are the thin red lines that surround the cell. Bar, 10 μm.

cells (Figure 2,A–D, left panels). In contrast, in cells expressing Rac1V12 (grown in the absence of DC), IgA was found not only in a centralized distribution characteristic of the ARE (Figure 2E) but also in the Rac1V12-positive aggregate (Figure 2F). In a kinetic analysis, we determined that basolaterally internalized IgA reached the central aggregate in as little as 5 min at 37°C (Leung, unpublished results). Moreover, entry of IgA into the central aggregate did not require passage through the apical plasma membrane (Leung, unpublished results). Little IgA was found concentrated at either the lateral or the basal membrane (Figure 2, G and H), indicating that internalized ligand had not been trapped in basolateral early endosomes. Rac1V12 was distributed at the lateral membrane and in a cluster at the very apex of the cell. In many, but not all, cells, Rac1V12 was also associated with the central aggregate, where it overlapped with punctate structures containing IgA (Figure 2E). Rac1V12 was also found in small punctate structures at the base of the cell (Figure 2H, left panel). There was no effect of Rac1N17 expression on the distribution of internalized IgA.

In addition to basolaterally internalized IgA, we observed that basolaterally internalized Tf was also highly concentrated in the central aggregate of Rac1V12-expressing cells (Figure 3, A–C). In fact, after a short pulse (10 min), the majority of the internalized Tf appeared within the central aggregate. Much, but not all, of the Tf within the aggregate colocalized with membranous elements containing basolaterally internalized IgA (Figure 3, A–C, arrows). Apically internalized IgA, a marker for the apical recycling pathway, was also delivered to the central aggregate within 15 min of being internalized (our unpublished results). In contrast to these early endosomal markers, the Ac17-positive compartments (predominantly late endosomes and lysosomes) were found to surround the IgA-positive central aggregate but were rarely seen to be incorporated into this structure (Figure 3, D–F). The distributions of these markers were unaltered in cells expressing Rac1N17.

Next, we assessed the distribution of marker proteins of the ER, Golgi, and TGN in cells expressing Rac1V12. In both control and Rac1V12-expressing cells, the ER resident protein mp30/BAP31 (Annaert *et al.*, 1997) was distributed throughout the cell cytoplasm, but in cells expressing Rac1V12, the ER was excluded from the region of the central aggregate (Figure 3, G–I). In control cells, giantin, a resident Golgi protein (Lindstedt and Hauri, 1993), was distributed in a ribbon-like structure that localized between the nucleus and the apical membrane. In Rac1V12-expressing cells, giantin-labeled Golgi appeared to be excluded from, and generally surrounded, the central aggregate (our unpublished results). In many cells, furin, a marker protein of the TGN (Molloy *et al.*, 1994), was excluded from the central aggregate (Figure 3, J–L), although an occasional furin-positive TGN ribbon was found within the central aggregate of some Rac1V12-expressing cells. The distributions of marker proteins of the ER and Golgi were unaffected in cells expressing Rac1N17.

The Central Aggregate Is Composed of Tubulovesicular Endosomal Elements

The ultrastructure of the central aggregate was examined at high resolution by electron microscopy. To mark the central aggregate, we internalized Fab fragments derived from affinity-purified antibodies to the secretory component coupled to HRP (Breitfeld *et al.*, 1989b). Like IgA, these Fab fragments move by transcytosis from the basolateral to the apical membrane (Breitfeld *et al.*, 1989b). In the presence of H_2O_2 and diaminobenzidine, HRP catalyzes the formation of a product that fills intracellular compartments and appears electron dense when examined by electron microscopy. In control cells, Fab-HRP was primarily localized to small tubulovesicular membrane elements in the apical cytoplasm, often beneath the apical membrane (Figure 4A). Note that the electron micrographs also show that control cells were relatively uniform in shape, with apical microvilli and few plasma membrane interdigitations of the lateral membrane.

In many cells expressing Rac1V12, Fab-HRP was located in tubulovesicular elements beneath the apical membrane, similar to those in control cells (Figure 4B). However, unlike in control cells, ligand was also found in the central aggregate (Figure 4, B and C). This is consistent with our confocal immunofluorescence analysis presented above (see Figure 2). In some Rac1V12-expressing cells, Fab-HRP labeled only the central aggregate, and little ligand was found underneath the apical membrane (Figure 4C). In electron micrographs, the central aggregate appeared as a heterogeneous cluster of small vesicular elements, tubules, signet ring–shaped structures, and occasionally a multivesicular body (Figure 4, B and C, insets). Many of these structures were labeled with the Fab-HRP, suggesting that they are endosomal in nature. This is consistent with our observation that these structures contain the endocytic marker rab11 (see Figure 8) (Jou and Nelson, 1998). In some sections, we found a centriole at the center of the aggregate (Figure 4B, inset). The presence of a centriole this deep in the cytoplasm is aberrant, because centrioles are usually located beneath the apical membrane, one of which forms the basal body for a single cilium that projects from the apical surface of the MDCK cell (Bacallao *et al.*, 1989). Although the localization of the central aggregate is aberrant, it is important to note that the organization (paracentriolar) and morphology of endosomal elements are similar to those observed previously in control cells (Parton *et al.*, 1989; Apodaca *et al.*, 1994).

In cells expressing Rac1V12, the Golgi apparatus was generally dispersed, and small Golgi stacks often surrounded the central aggregate (Figure 4C). This is consistent with our confocal immunofluorescence analysis of giantin and furin distributions (see Figure 3, J–L). However, Golgi were rarely found within the aggregate. Several other structural features of Rac1V12 cells were different from those of control cells (Figure 4B). Occasionally, we observed that the aggregate was surrounded by bundles of thin (10-nm) filaments (Figure 4C), presumably intermediate filaments. In cross-section, the profile of Rac1V12 cells was tortuous, with a small diameter at the apex of the cell and a progressively wider diameter at the base of the cell, or vice versa. There was an occasional cell that grew on top of its neighbors. In general, cells had few microvilli, and those present were sometimes fused with adjacent microvilli. One of the most pronounced effects of Rac1V12 expression was the dramatic increase in membrane interdigitations in the lateral membranes between adjacent cells.

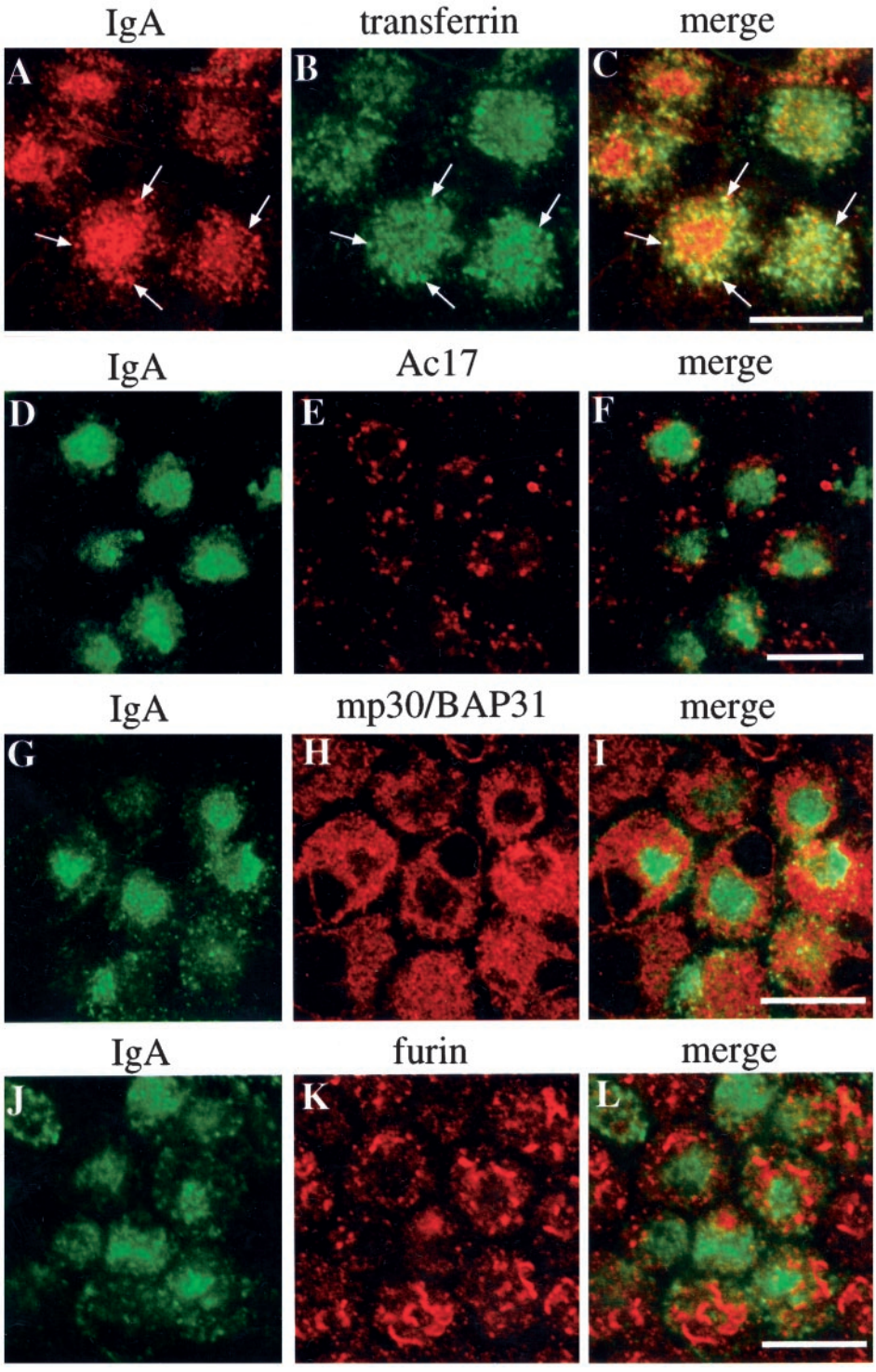

Figure 3. Distribution of IgA, Tf, the Ac17 antigen, mp30/BAP31, and furin in cells expressing Rac1V12. IgA was internalized from the basolateral surface of the cell for 10 min at 37°C, washed, and then chased for 60 min at 37°C. (A–C) Tf was internalized during the last 10 min of the 60-min chase. The cells were fixed, incubated with antibodies against IgA and Tf (A–C), IgA and Ac17 antigen (D–F), IgA and mp30/BAP31 (G–I), or IgA and furin (J–L) and then reacted with the appropriate secondary antibody coupled to FITC or Cy5. Arrows indicate regions of colocalization. A single optical section at the level of the central aggregate was obtained with a scanning laser confocal microscope. Bar, 10 μm.

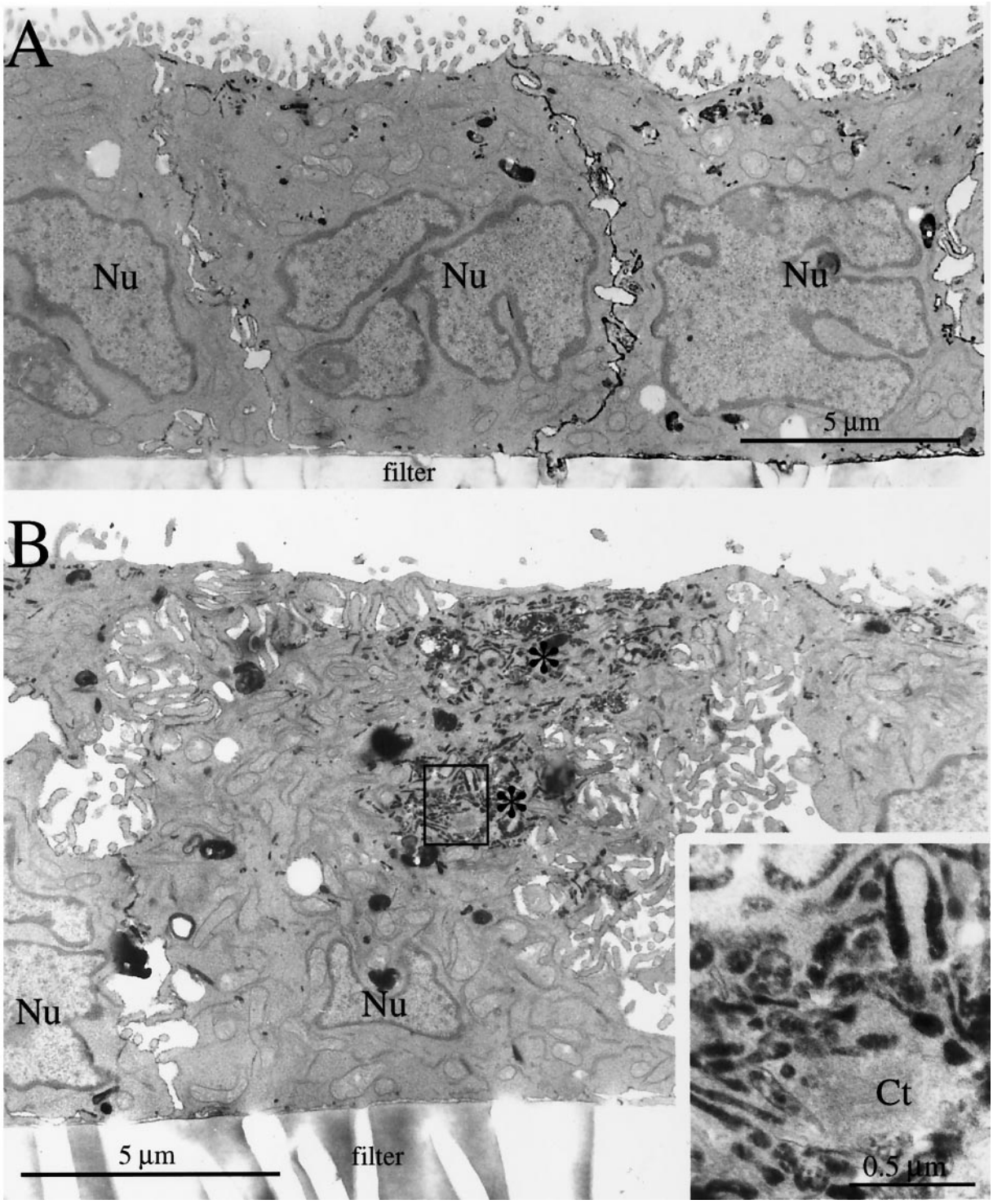

Figure 4. Ultrastructural analysis of Rac1V12 cells grown in the presence or absence of DC. Fab-HRP was internalized from the basolateral pole of the cell, the cells were fixed, a DAB reaction was performed, and the cells were processed for electron microscopy. (A) Cells grown in the presence of DC. (B) Cells grown in the absence of DC. Clusters of Fab-HRP–labeled structures are labeled with asterisks. The upper cluster represents ligand present in the common endosome/ARE, and the bottom cluster represents ligand present in the central aggregate. (Inset) A magnified view of the endosomal elements that constitute the central aggregate. Ct, centriole. (C) Cells grown in the absence of DC. A juxtanuclear central aggregate is shown. (Inset) A magnified view of the 10-nm filaments surrounding the endosomal elements of the central aggregate (marked with arrows). G, Golgi stacks; LF, infoldings of the lateral membrane; Nu, nucleus.

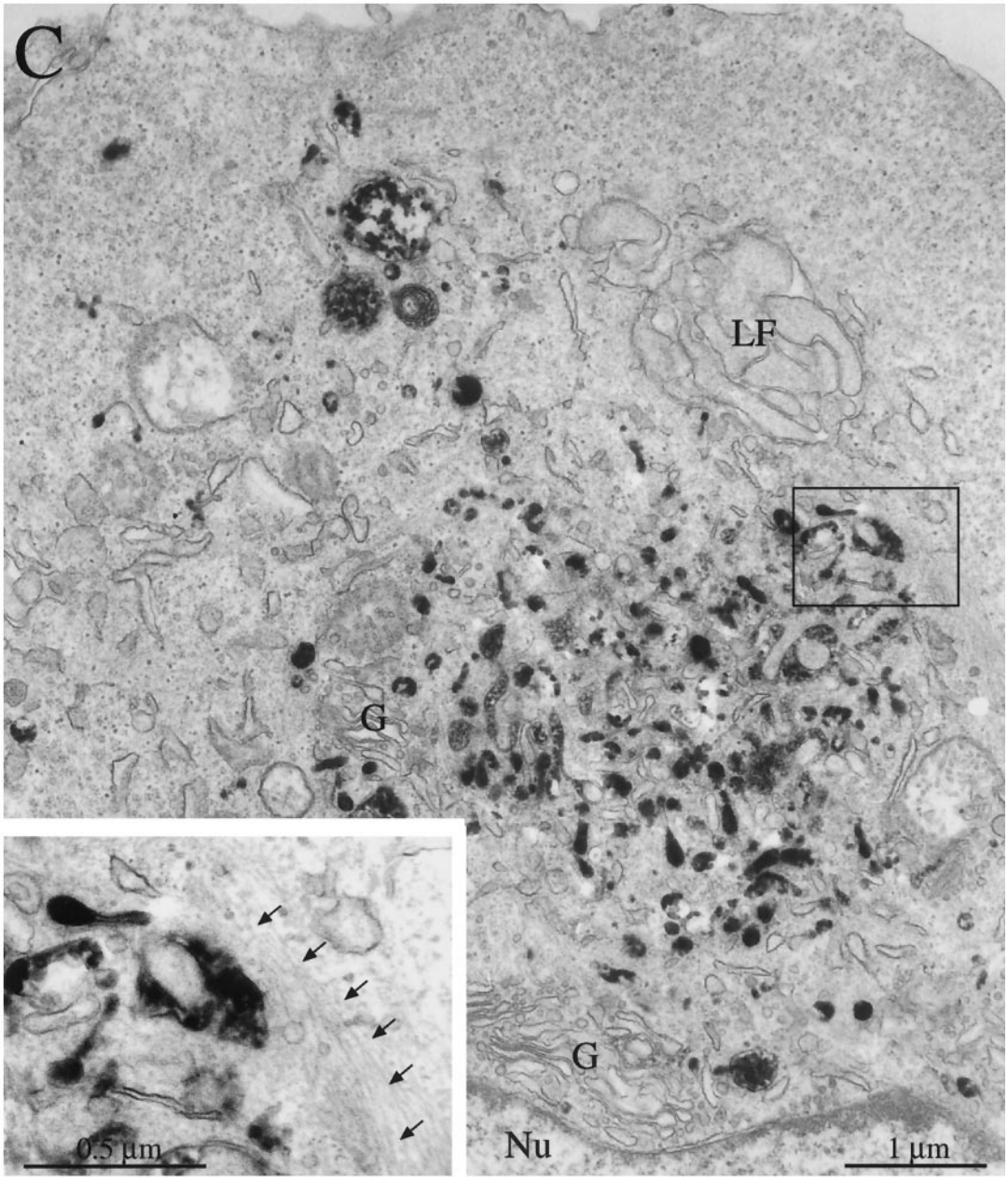

Figure 4 (Cont.)

Rates of Apical and Basolateral Endocytosis Are Affected by Mutant Rac1 Expression

Rac1 is known to affect pinocytosis in oocytes and receptor-mediated endocytosis in HeLa cells (Schmalzing *et al.*, 1995; Lamaze *et al.*, 1996). To determine whether Rac1 mutants affected endocytosis in MDCK cells, we measured the rate of [^{125}I]IgA internalization from either the apical or the basolateral membrane. In cells expressing Rac1V12, the rate of both apical and basolateral endocytosis of [^{125}I]IgA was decreased by ~30% (Figure 5, A and C). In contrast, Rac1N17 expression increased the rate of apical and basolateral endocytosis (Figure 5, B and D). The Rac1N17 effect on apical endocytosis was especially pronounced, with a two- to threefold increase in the rate at early times. The rate and extent of basolateral endocytosis was enhanced by Rac1N17 expression at all times.

Apically Directed Postendocytic Traffic Is Impaired in Rac1V12-expressing Cells

The finding that endocytosed ligands were delivered to the central aggregate in Rac1V12-expressing cells prompted us to explore whether postendocytic traffic was altered in these cells and in cells expressing Rac1N17. In the assays described below, we measured transcytotic delivery of ligands

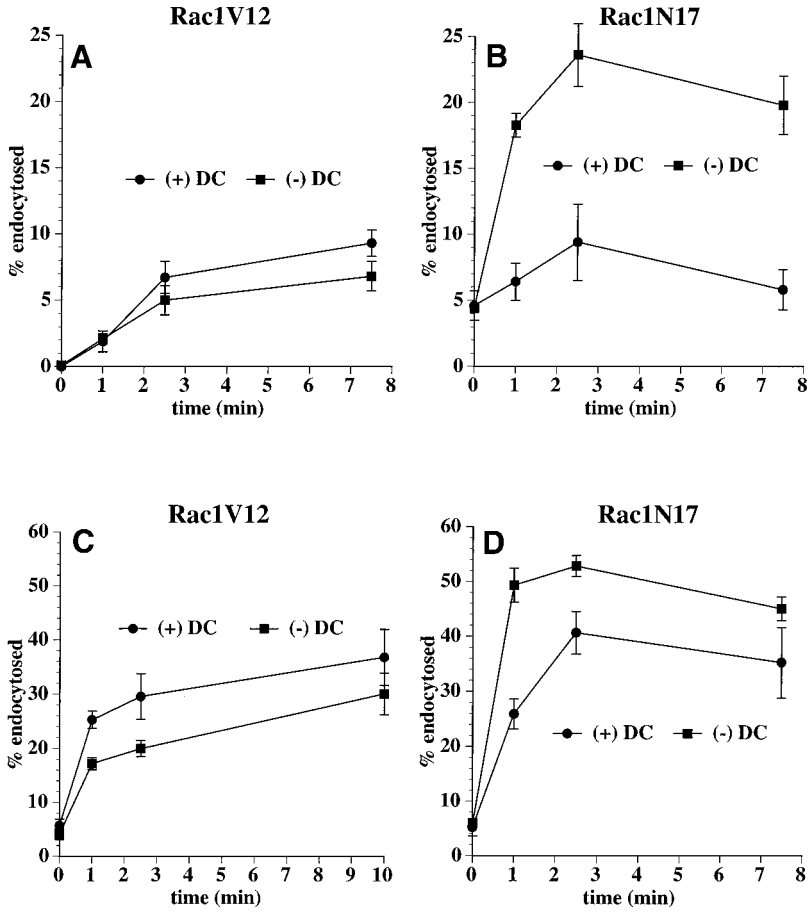

Figure 5. Apical and basolateral endocytosis in Rac1V12 and Rac1N17 cells. [^{125}I]IgA was bound to the apical (A and B) or basolateral (C and D) surface of cells for 60 min at 4°C. The Rac1V12 (A and C) or Rac1N17 (B and D) cells were washed and then incubated at 37°C for the times indicated. The media were collected, and the cells were then rapidly cooled on ice. [^{125}I]IgA was stripped from the cell surface by a sequential treatment with trypsin and acid at 4°C, and the filters were cut out of their holders. Total [^{125}I]IgA initially bound to the cells included ligand released into the medium, ligand stripped from the cell surface with trypsin and acid, and cell-associated ligand not sensitive to stripping (endocytosed) and was quantified with a gamma counter. Shown is the percentage of total endocytosed ligand from a representative experiment (mean ± SD; n = 3).

from the basolateral to the apical membrane by sampling medium in the appropriate compartment of confluent monolayers grown on Transwell filters. However, we had demonstrated previously that tight junction function is altered in cells expressing Rac1V12 and Rac1N17, and as a result, the paracellular flux of several markers is increased (Jou *et al.*, 1998). Because large-scale paracellular diffusion of ligands between the apical and basolateral compartments could significantly alter the interpretation of our results, we determined the extent of [^{125}I]IgA and [^{125}I]Tf flux in Rac1V12-expressing cells. Although there was an increase in paracellular flux, <1.2% of apically added [^{125}I]IgA or [^{125}I]Tf appeared in the basolateral compartment of the cells after 60 min at 37°C (our unpublished results). This small increase in flux was insufficient to alter the outcome of the postendocytic fate assays described below. Similar results were observed in cells expressing Rac1N17.

The fate of basolaterally internalized [^{125}I]IgA in control and Rac1V12-expressing cells is shown in Figure 6A. In control cells, ~85% of ligand was transcytosed and released into the apical medium during a 2-h chase, ~8% of ligand was released back into the basolateral compartment, ~5% was degraded, and ~2% remained in the cell. These results are similar to those published previously (Apodaca *et al.*, 1994). In cells expressing Rac1V12, transcytosis of internalized [^{125}I]IgA to the apical compartment was decreased by 45–50% (Figure 6A). This decrease was not accounted for by the small changes in the amount of ligand released basolaterally and the amount of ligand degraded. However, the decrease could be accounted for by the ~15-fold increase in the amount of ligand that remained cell associated (29% in Rac1V12-expressing cells, compared with 2% in control cells). Rac1N17 expression had little or no effect on the postendocytic fate of basolaterally internalized [^{125}I]IgA (Figure 6B).

To determine the compartment(s) in which cell-associated IgA was trapped in Rac1V12-expressing cells, IgA was internalized for 10 min and then chased for 60 min at 37°C, during which time most of the ligand was released into the apical secretions of control cells. Cells were processed for immunofluorescence, and the samples were examined by confocal microscopy. In control cells, the amount of detectable cell-associated ligand was very small. In cells expressing Rac1V12, however, internalized IgA strongly labeled the central aggregate (Figure 6, C and D). In some cells, IgA was also found under the apical plasma membrane in the ARE (Figure 6C, arrow). Taking these kinetic and morphological data together, we conclude that in the presence of Rac1V12, delivery of ligand to the central aggregate is efficient but exit of IgA from this compartment is inefficient.

The fate of apically internalized [^{125}I]IgA was also assessed in cells expressing Rac1V12 or Rac1N17. Although

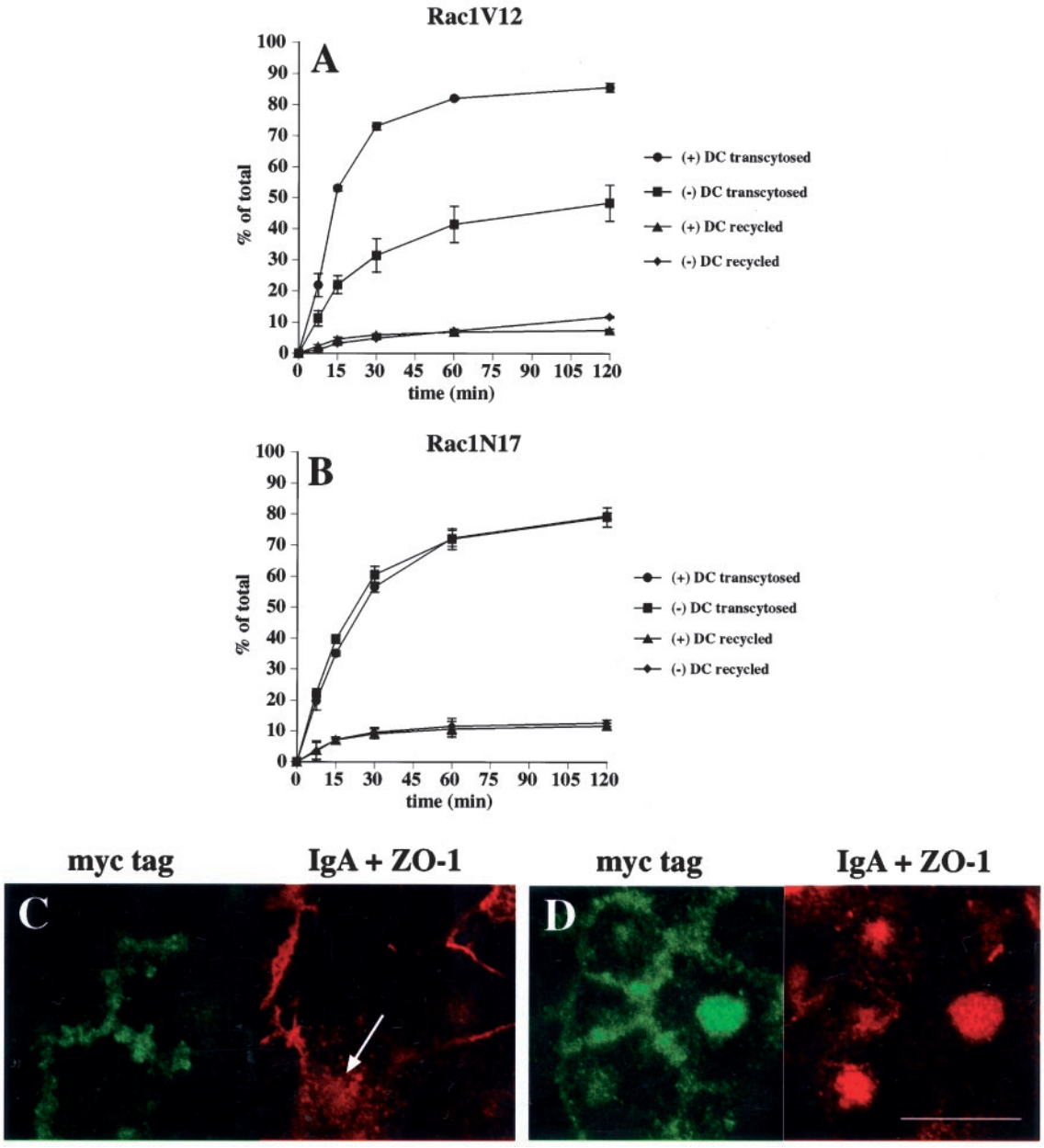

Figure 6. Postendocytic fate of basolaterally internalized IgA in Rac1V12- and Rac1N17-expressing cells. [^{125}I]IgA was internalized from the basolateral surface of the cells for 10 min at 37°C, and the cells were washed and then chased for 120 min. The percentage of total ligand released apically (transcytosed) or basolaterally (recycled) in cells expressing Rac1V12 (A) or Rac1N17 (B) is shown. Values for degradation were as follows: Rac1V12 + DC, 5.0 ± 0.7%; Rac1V12 − DC, 10.6 ± 0.7%; Rac1N17 + DC, 5.6 ± 0.3%; Rac1N17 − DC, 4.4 ± 0.5%. Values for ligand remaining cell associated were as follows: Rac1V12 + DC, 2.0 ± 0.7%; Rac1V12 − DC, 29.1 ± 6.7%; Rac1N17 + DC, 3.1 ± 0.2%; Rac1N17 − DC, 3.8 ± 1.0%. Values (mean ± SD; n = 3) are from a representative experiment. (C and D) IgA was internalized from the basolateral cell surface for 10 min at 37°C, and the cells were washed and then chased for 60 min at 37°C in ligand-free medium. The cells were fixed, incubated with antibodies against myc-tagged Rac1V12, IgA, and ZO-1, and then reacted with the appropriate secondary antibody coupled to FITC or Cy5. Single optical sections at the level of the tight junctions (C) or the central aggregate (D) were obtained with a scanning laser confocal microscope. The arrow in C demarks a cell in which some IgA is seen accumulating at the apical pole of the cell. Bar, 10 μm.

pIgR is efficiently cleaved at the apical pole of MDCK cells to produce a secretory component, a fraction of the receptor escapes cleavage and can be internalized with ligand from the apical cell surface (Breitfeld *et al.*, 1989b). The majority of this apically internalized pool of pIgR-IgA is then recycled back to the apical membrane. In Rac1V12 cells, the amount of internalized ligand that was recycled to the apical membrane was reduced by ~30% (Figure 7A). We detected little

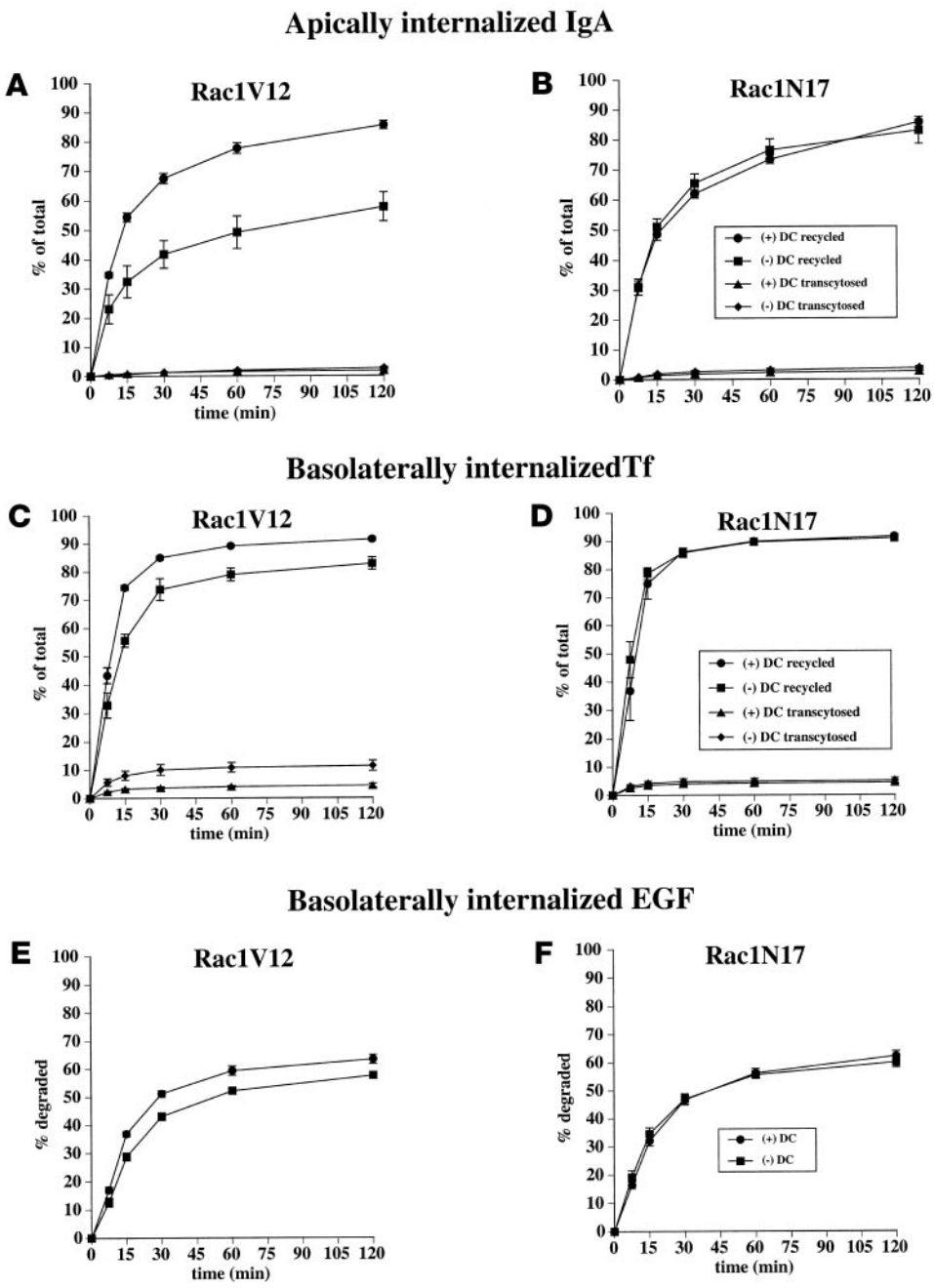

Figure 7. Postendocytic fate of apically internalized IgA, basolaterally internalized Tf, and basolaterally internalized EGF in cells expressing Rac1V12 or Rac1N17. (A and B) [^{125}I]IgA was internalized from the apical surface of the cells for 10 min at 37°C, and the cells were washed and then chased for 120 min. The percentage of total ligand released apically (recycled) or basolaterally (transcytosed) in cells expressing Rac1V12 (A) or Rac1N17 (B) is shown. Values for degradation were as follows: Rac1V12 + DC, 7.6 ± 0.7%; Rac1V12 − DC, 11.3 ± 1.1%; Rac1N17 + DC, 7.3 ± 0.3%; Rac1N17 − DC, 5.2 ± 0.4%. Values for ligand remaining cell associated were as follows: Rac1V12 + DC, 5.1 ± 0.9%; Rac1V12 − DC, 28.3 ± 4.8%; Rac1N17 + DC, 4.3 ± 0.7%; Rac1N17 −DC, 7.8 ± 3.9%. Values (mean ± SD; n = 3) are from a representative experiment. (C and D) [^{125}I]Tf was internalized from the basolateral surface of the cells for 30 min at 37°C, and the cells were washed and then chased for 120 min at 37°C. The percentage of total ligand released apically (transcytosed) or basolaterally (recycled) in cells expressing Rac1V12 (C) or Rac1N17 (D) is shown. Values for degradation were as follows: Rac1V12 + DC, 2.8 ± 0.1%; Rac1V12 − DC, 2.8 ± 0.1%; Rac1N17 + DC, 2.2 ± 0.3%; Rac1N17 − DC, 1.7 ± 0.2%. Values for ligand remaining cell associated were as follows: Rac1V12 + DC, 1.8 ± 0.2%; Rac1V12 − DC, 3.1 ± 0.4%; Rac1N17 + DC, 1.8 ± 0.6%; Rac1N17 − DC, 2.3 ± 0.6%. Values (mean ± SD; n = 4) are from a representative experiment. (E and F) [^{125}I]EGF was internalized from the basolateral surface of the cells for 10 min at 37°C, and the cells were washed and then chased for 120 min. The percentage of total degraded ligand in cells expressing Rac1V12 (E) or Rac1N17 (F) is shown. Values for transcytosis were as follows: Rac1V12 + DC, 8.7 ± 0.7%; Rac1V12 − DC, 11.5 ± 0.8%; Rac1N17 + DC, 10.0 ± 1.2%; Rac1N17 − DC, 12.1 ± 1.0%. Values for ligand recycling were as follows: Rac1V12 + DC, 22.8 ± 1.7%; Rac1V12 − DC, 24.6 ± 0.8%; Rac1N17 + DC, 21.5 ± 0.8%; Rac1N17 − DC, 22.6 ± 1.1%. Values for ligand remaining cell associated were as follows: Rac1V12 + DC, 5.2 ± 0.5%; Rac1V12 − DC, 6.6 ± 0.5%; Rac1N17 + DC, 5.3 ± 1.0%; Rac1N17 − DC, 5.4 ± 1.0%. Values (mean ± SD; n = 4) are from a representative experiment.

or no effects on either apical-to-basolateral transcytosis or intracellular degradation of apical internalized ligand. However, we detected a five- to sixfold increase in the amount of cell-associated ligand in Rac1V12 cells compared with controls. Confocal microscopy confirmed that cell-associated ligand was trapped in the central aggregate of cells expressing Rac1V12. There was no effect of Rac1N17 expression on the postendocytic traffic of apically internalized [^{125}I]IgA (Figure 7B).

Next, we examined whether the postendocytic fates of a basolateral recycling marker (Tf) and a marker of the degradative pathway (EGF) were affected in Rac1V12- or

Rac1N17-expressing cells. Recycling of basolaterally internalized [^{125}I]Tf was decreased slightly in cells expressing Rac1V12 (Figure 7C) and was coupled with an increase in the amount of ligand released from the apical membrane (~11% in Rac1V12-expressing cells, compared with ~5% in control cells). In contrast to basolaterally internalized IgA, there was little difference in the amount of [^{125}I]Tf degraded (~3%) or cell associated (2–3%) between control cells and cells expressing Rac1V12. These results indicate that proteins that recycle to the basolateral membrane may be able to efficiently exit the central aggregate. To confirm this observation, we cointernalized Tf and IgA for 10 min at 37°C and then followed the kinetics of Tf exit from the IgA-labeled central aggregate with the use of indirect immunofluorescence. As shown in Figure 3, we observed colocalization of the two markers after the pulse. However, within 30 min of chase, there was no detectable Tf associated with the IgA-labeled central aggregate (our unpublished results). There was no effect of Rac1N17 expression on [^{125}I]Tf recycling (Figure 7D).

When [^{125}I]EGF was internalized from the basolateral surface of control cells, ~60% of ligand was degraded (Figure 7E), ~25% was recycled to the basolateral membrane, ~10% was transcytosed, and the remainder was cell associated. Rac1V12 expression slightly decreased the amount of [^{125}I]EGF that was degraded (Figure 7E) and slightly increased the amounts of ligand released from the apical and basolateral membranes. There was no increase in the amount of [^{125}I]EGF that was cell associated in cells expressing Rac1V12. Rac1N17 expression had no effect on the postendocytic traffic of [^{125}I]EGF (Figure 7F).

Protein Exit from the Central Aggregate in Rac1V12 Cells Is Unaffected by Nocodazole but Is Enhanced by Disruption of the Actin Cytoskeleton by CD

The paracentriolar distribution of the central aggregate indicated that its organization might be dependent on the integrity of the microtubule cytoskeleton. To test this possibility, we treated cells with nocodazole, a microtubule-depolymerizing agent. This treatment resulted in a complete dispersion of the central aggregate; immunofluorescence showed that rab11 and myc-tagged Rac1V12 were localized to small puncta that were dispersed throughout the apical cytoplasm (Figure 8, compare A and B with C and D).

Because ligand that was delivered to the central aggregate in Rac1V12 cells did not efficiently exit this structure, we asked whether dispersal of the aggregate with nocodazole would restore normal protein trafficking from the central aggregate to the apical membrane. To load the central aggregate with [^{125}I]IgA, Rac1V12-expressing cells were pulse labeled with [^{125}I]IgA for 10 min, followed by a 60-min chase to allow [^{125}I]IgA to accumulate in the central aggregate (as shown above). The cells were then chilled to 4°C and either left untreated or incubated in the presence of nocodazole. The fate of this intracellular cohort of ligand was then measured during a 2-h chase period at 37°C in the continued presence of nocodazole (Figure 8E). Exit of [^{125}I]IgA from the central aggregate was similarly slow in untreated cells and cells treated with nocodazole. These results indicate that dispersal of the central aggregate with nocodazole is not sufficient to restore normal endocytic function in Rac1V12-expressing cells.

We next tested the effect of disruption of the actin cytoskeleton with CD on protein trafficking out of the central aggregate. Although there appeared to be little effect of CD on the organization or distribution of the central aggregate, CD treatment caused the release of trapped ligand and a significant increase in the amount of IgA that was released into the apical compartment (Figure 8F). This observation suggests that the trapping function of this aberrant compartment may be attributable in part to Rac1V12-induced changes in the actin cytoskeleton.

Delivery of Newly Synthesized Membrane Proteins to the Apical, but Not the Basolateral, Membrane Is Decreased in Rac1V12-expressing MDCK Cells

Previously, we showed that the apical membrane protein GP-135 was present in the central aggregate in cells expressing Rac1V12 (Jou and Nelson, 1998). Therefore, we explored whether this aberrant localization was the result of a block in biosynthetic traffic of GP-135 between the Golgi and the apical membrane. Cells were pulse labeled with [^{35}S]met/cys for 15 min and chased for different times up to 240 min, and plasma membrane delivery of newly synthesized GP-135 was assessed by cell surface biotinylation. In control cells, newly synthesized GP-135 was rapidly delivered to the apical membrane (Figure 9, A and B). In cells expressing Rac1V12, the initial delivery of GP-135 to the apical membrane was identical to that observed in control cells, but the amount of GP-135 that accumulated at the apical plasma membrane was decreased by ~75% (Figure 9, A and B). Under both conditions, GP-135 was completely solubilized in buffer containing Triton X-100, suggesting that it had not become aggregated into a detergent-insoluble complex. By following the internalization of a biotinylated cohort of GP-135, we determined that the lack of accumulation of GP-135 at the apical plasma membrane was not the result of increased endocytosis of GP-135 from the apical pole of the cell; in control and Rac1V12-expressing cells, <5% of cell surface GP-135 was internalized per hour (our unpublished results). These data indicate that a small fraction of GP-135 was rapidly delivered to the apical cell surface of Rac1V12-expressing cells, whereas the remainder was retained inside the cell, presumably in the central aggregate. Note that, as in our previous studies (Grindstaff *et al.*, 1998a), we found that <5% of newly synthesized GP-135 was delivered to the basolateral membrane in either control cells or cells expressing Rac1V12, and these data are not shown here.

We also measured delivery of newly synthesized pIgR to the basolateral membrane of control cells and cells expressing Rac1V12 or Rac1N17. As described previously, the majority of newly synthesized pIgR is delivered directly to the basolateral membrane (Casanova *et al.*, 1991; Aroeti *et al.*, 1993). We did not observe a significant difference in basolateral delivery of the pIgR between control cells and cells expressing Rac1V12 (Figure 9C). However, Rac1N17 expression decreased delivery of the pIgR to the basolateral membrane by ~20%.

DISCUSSION

An initial characterization of cells expressing Rac1V12 revealed that a central aggregate formed beneath the apical

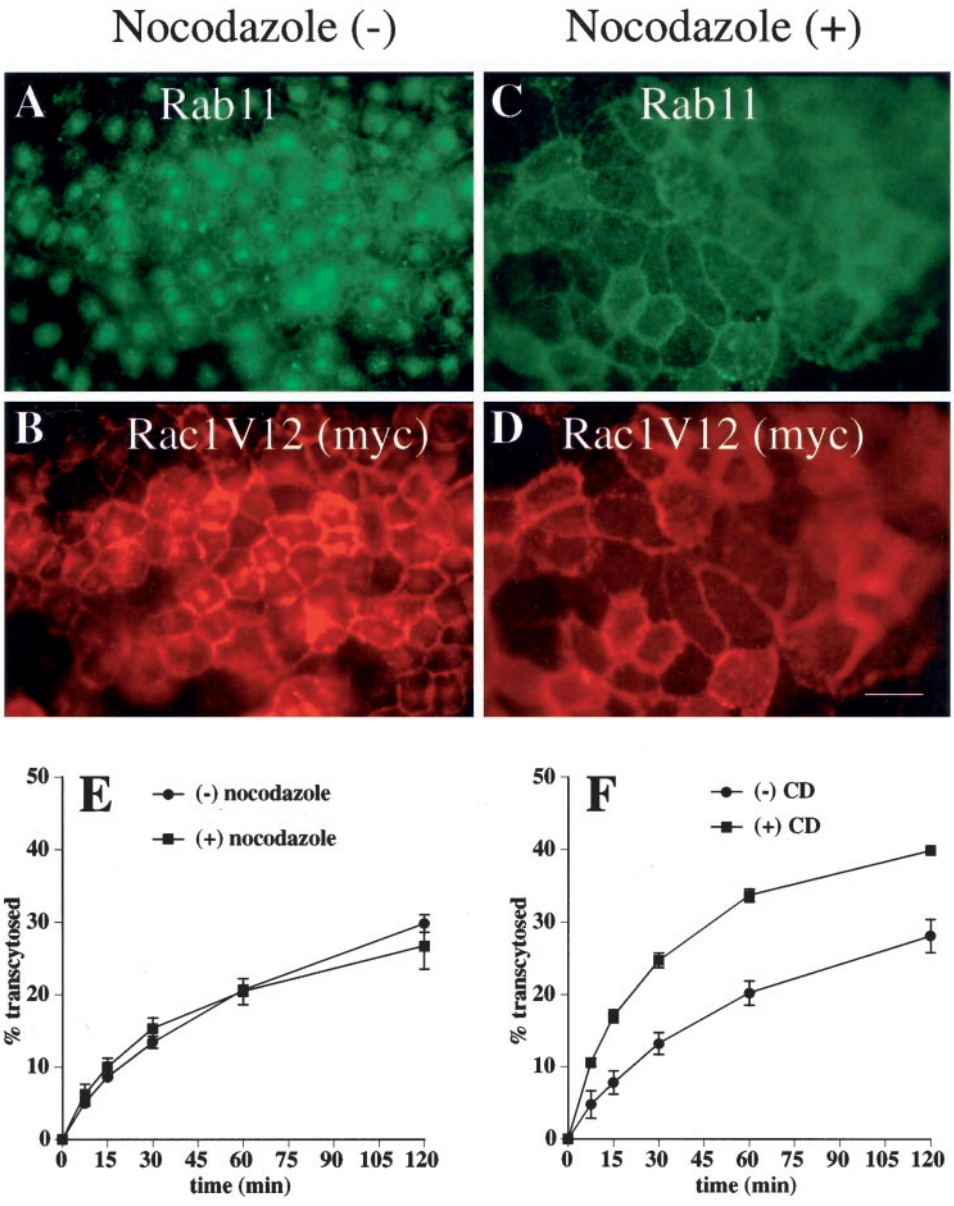

Figure 8. Effects of nocodazole and CD on the distribution and exit of proteins from the central aggregate. (A–D) Cells were mock treated or treated with nocodazole, fixed, incubated with antibodies against rab11 and the myc tag, and then reacted with the appropriate secondary antibody coupled to FITC or Texas red. Bar, 10 μm. (E) [^{125}I]IgA was internalized from the basolateral surface of the cells for 10 min at 37°C, and the cells were washed and then chased for 60 min. Cells were rapidly chilled to 4°C for 60 min (with [+] or without [−] nocodazole), and the postendocytic fate of ligand was assessed in a subsequent 120-min incubation at 37°C (with or without nocodazole). The percentage of total ligand released apically (transcytosed) is shown. Values for degradation were as follows: without nocodazole, 21.0 ± 1.2%; with nocodazole, 21.9 ± 0.8%. Values for ligand remaining cell associated were as follows: without nocodazole, 36.1 ± 5.5%; with nocodazole, 37.2 ± 1.5%. (F) [^{125}I]IgA was internalized from the basolateral surface of the cells for 10 min at 37°C, and the cells were washed and then chased for 45 min at 37°C. After a 15-min treatment with (+) or without (−) 25 μg/ml CD, the postendocytic fate of ligand was assessed in a 120-min incubation at 37°C (with or without CD). The percentage of total ligand released apically (transcytosed) is shown. Values for degradation were as follows: without CD, 10.2 ± 0.5%; with CD, 14.0 ± 1.1%. Values for ligand remaining cell associated were as follows: without CD, 46.7 ± 2.2%; with CD, 35.7 ± 1.1%. Values (mean ± SD; n = 3) are from a representative experiment.

membrane (Jou and Nelson, 1998). To investigate the nature of this aggregate, we have performed a detailed analysis of endocytic and biosynthetic trafficking pathways in these cells. We have found that activation of Rac1 has multiple downstream effects on many membrane trafficking events in polarized cells, including apical and basolateral endocytosis, basolateral-to-apical transcytosis, apical recycling, and accumulation of newly synthesized membrane proteins at the apical cell surface.

Rac1 Regulates the Plasma Membrane Endocytic Rate

Recent evidence indicates that Rho family members are important regulators of endocytosis, because mutants of either RhoA or Rac1 alter fluid-phase and receptor-mediated endocytosis in nonpolarized cells (Schmalzing *et al.*, 1995; Lamaze *et al.*, 1996). In MDCK cells, RhoA appears to be an important modulator of both apical and basolateral endocytosis (Leung *et al.*, 1999). Our current results show that endocytosis from both plasma membrane domains of polarized MDCK cells was decreased by Rac1V12 and increased by Rac1N17. These observations indicate that Rac1 may act as a throttle on the rate of endocytosis, with the GTP-bound form decreasing the rate and the GDP form increasing the rate. These results are consistent with the Rac1-mediated regulation of receptor-mediated endocytosis reported in nonpolarized HeLa cells by Lamaze *et al.* (1996) but are in contrast to those of Li *et al.* (1997), who found no effect of

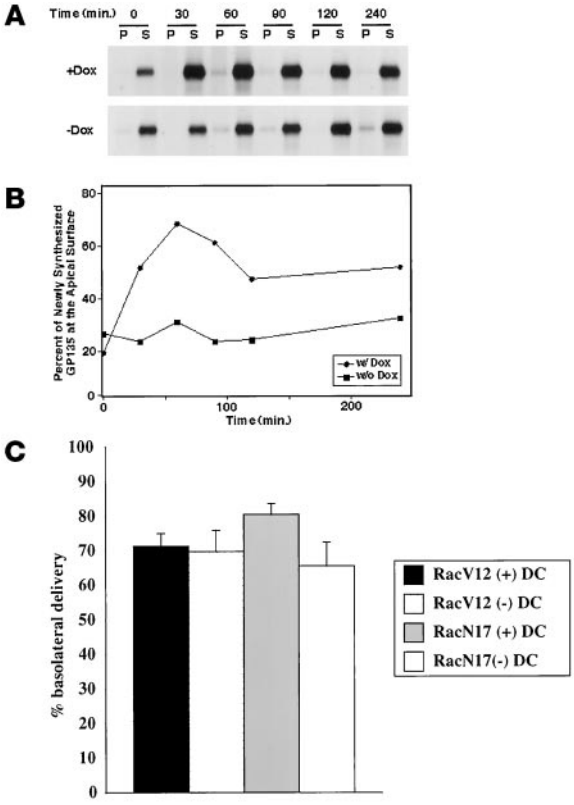

Figure 9. Effect of Rac1V12 expression on trafficking of newly synthesized apical proteins from the Golgi complex to the cell surface. (A and B) MDCK cells were grown in the presence (+) or absence (−) of DC (Dox) on Transwell filters. Cells were metabolically labeled for 15 min with [^{35}S]met/cys and then chased for different times in medium containing an excess of unlabeled met/cys. For analysis of GP-135 trafficking, pairs of filters were processed for apical (A) and basolateral (B) cell surface biotinylation. Cells were extracted with buffer containing Triton X-100 to yield soluble (S) and insoluble (P) fractions, from which the biotinylated fraction of GP-135 was isolated by sequential GP-135 antibody and streptavidin-agarose precipitation. A separate filter for each time point was extracted with SDS lysis buffer, and GP-135 was immunoprecipitated directly to obtain the total amount of [^{35}S]met/cys-labeled GP-135 in the cells. Proteins were separated by SDS-PAGE and detected subsequently with the use of a Molecular Dynamics (Sunnyvale, CA) PhosphorImager (see MATERIALS AND METHODS) (Grindstaff *et al.*, 1998a). Kinetics of GP-135 (A and B) trafficking to the apical membrane domain are presented. Data are from a representative experiment. As shown by us previously, <5% of GP-135 is delivered to the basolateral membrane in control cells (Grindstaff *et al.*, 1998a) and Rac1V12 cells (Fung, unpublished results); these data, therefore, are not presented. To determine the proportion of GP-135 on the apical membrane, the amount of apical biotinylated GP-135 was divided by the total amount of labeled GP-135 in the cell, and the fraction was plotted against the time of the chase (B). (C) Cells were metabolically labeled with [^{35}S]cys for 15 min at 37°C and then chased in the presence (+) or absence (−) of basolateral trypsin for 60 min at 37°C, as described previously (Apodaca *et al.*, 1993; Aroeti and Mostov, 1994). In the presence of trypsin, newly synthesized pIgR delivered to the basolateral cell surface was rapidly proteolyzed. By comparing the amount of immunoprecipitable pIgR in non-trypsin-treated cells and cells treated with trypsin, it is possible to quantify the extent of pIgR delivery to the basolateral cell surface (Apodaca *et al.*, 1993; Aroeti and Mostov, 1994). The percentage of basolateral delivery is shown (mean ± SD; n = 4).

dominant active Rac1 expression on fluid-phase endocytosis in baby hamster kidney cells. This discrepancy may reflect differences in cell type or the use of a fluid phase marker by Li *et al.* and ligands that undergo receptor-mediated endocytosis in our study and that of Lamaze *et al.*

Expression of Rac1V12 Alters Delivery of Proteins to the Apical Membrane of MDCK Cells

Although there have been several reports of Rho family members regulating endocytosis and exocytosis (Norman *et al.*, 1994, 1996; Price *et al.*, 1995; Schmalzing *et al.*, 1995; Lamaze *et al.*, 1996; Mariot *et al.*, 1996; O'Sullivan *et al.*, 1996; Brown *et al.*, 1998; Kroschewski *et al.*, 1999), little is known about the roles of these proteins in postendocytic or biosynthetic traffic. In cells expressing Rac1V12, we observed that apically directed membrane protein traffic was selectively impaired compared with traffic directed toward the basolateral membrane. Both basolateral-to-apical transcytosis and the apical recycling pathway were significantly altered in cells expressing Rac1V12. Significantly, alterations of these apically directed pathways appeared to be the direct result of the delivery to, and the retention of, these proteins in the central aggregate. In contrast, basolateral recycling of Tf and delivery of EGF to late endosomes/lysosomes were less perturbed by Rac1V12 expression. Although Tf was delivered to the central aggregate, it was not retained in this compartment and was recycled reasonably efficiently to the basolateral pole of the cell. This observation indicates that sorting machinery in the aggregate for basolaterally targeted proteins remained intact in these Rac1V12-expressing cells.

To determine if TGN-to-cell surface delivery was altered in Rac1V12 cells, we measured the appearance of newly synthesized GP-135 and the pIgR at the apical and basolateral plasma membranes, respectively. Delivery of the pIgR to the basolateral membrane was unimpaired in Rac1V12-expressing cells. However, accumulation of newly synthesized GP-135 at the apical plasma membrane domain was decreased by ~75%. Note that the remaining GP-135 was not delivered to the basolateral membrane but was retained inside the cells. Presumably, this intracellular pool of GP-135 was delivered to and/or retained in the central aggregate, where the protein accumulated to high levels. At present, we do not know whether delivery of GP-135 to the central aggregate is a result of direct delivery from the TGN and trapping or a result of aberrant redistribution of GP-135 from another cellular membrane as a consequence of Rac1V12 expression. We do not believe that increased apical endocytosis accounts for the decreased accumulation of GP-135 at the apical surface of cells expressing Rac1V12, because <5.0% of cell surface GP-135 was endocytosed per hour in these cells.

Rac1V12 expression had dramatic effects on slowing apically directed biosynthetic or postendocytic traffic, whereas Rac1N17 expression had little effect on these trafficking pathways. This was surprising because it was expected that Rac1N17 expression would act as an antagonist to the effects of Rac1V12, as we found in the case of the rate of endocytosis (see above). We have observed previously that this level of Rac1N17 expression (approximately five times greater than that of endogenous Rac1) is sufficient to alter cellular polarity (Jou and Nelson, 1998), decrease transepithelial resistance (Jou *et al.*, 1998), and increase the rate of

endocytosis (see above). As such, the role of Rac1 in the normal function of these postendocytic trafficking pathways is unclear at present. It was observed recently that other dominant negative mutants of small GTPases (e.g., rab25) have little effect on endocytic traffic out of the ARE (Casanova *et al.*, 1999), and a dominant negative mutant of the early endosome-associated GTPase RhoD has no effect on endosome morphology or function (Murphy *et al.*, 1996). Perhaps the traffic of proteins from the ARE to the apical surface is modulated only by changes in the activation of these small GTPases. This would be similar to the effects of protein kinase C and protein kinase A on postendocytic traffic; when activated, these kinases modulate apically directed traffic, whereas inactivation of these kinases apparently has no effect (Cardone *et al.*, 1994; Hansen and Casanova, 1994).

Membrane and Protein Accumulation in the Central Aggregate Is Due, in Part, to Alterations in the Actin Cytoskeleton

Although the role of Rac1 in normal postendocytic traffic is somewhat unclear, our data indicate that the central aggregate observed in Rac1V12-expressing cells does not constitute a random assortment of membranes from different organelles or trafficking pathways. Instead, it contains specific membranes and proteins that are blocked in their exit to the apical membrane. Marker proteins of late endosomes/lysosomes, the Golgi, the TGN, and the ER were not found within the aggregate. Electron microscopy revealed that it is composed of membranous structures, including vesicular elements, tubules, and signet ring–shaped structures, that are redolent of early endosomes. rab11, a marker of recycling endosomes in general and the ARE in particular (an early endosomal compartment) (Ullrich *et al.*, 1996; Ren *et al.*, 1998; Casanova *et al.*, 1999), was found to be associated with the central aggregate. The presence of Tf in the central aggregate indicates that the central aggregate is composed in part of common endosomal elements. Under normal conditions, the balance between membrane entry into and exit from the endosome results in the maintenance of a small resident pool of membranes in this structure. Inhibition of membrane exit from the ARE/common endosome by Rac1V12 may result in a proportional increase in the amount of resident membrane and formation of the central aggregate. As such, Rac1V12 expression may be a useful tool to understand the normal requirements for protein exit from the ARE/common endosome.

What is the underlying mechanism for the retention of apically directed cargo in cells expressing Rac1V12? One possible explanation is that apically directed traffic is prevented from exiting the central aggregate because of interactions between endosomes or endocytic transport vesicles and the surrounding cytoskeletal cage of filamentous actin and cytokeratin intermediate filaments. Although elements of the central aggregate were organized around a centriole, dispersal of the central aggregate by nocodazole did not relieve the block in protein exit to the apical membrane. In contrast, CD-induced disruption of the actin cytoskeleton restored the ability of some ligand to exit the cell. This observation suggests that some of the defects in postendocytic traffic may be the result of Rac1V12-promoted actin polymerization.

An alternative or additional possibility is that Rac1V12 exerts its effects by acting on effector pathways that are independent of its action on the actin cytoskeleton. Potential downstream effectors that are activated by Rac1 include RhoA, phospholipase D, phosphoinositol-4-phosphate 5-OH kinase, phosphatidylinositol-3-kinase (PI-3-K), PAK, and POR1 (reviewed by Van Aelst and D'Souza-Schorey, 1997). We believe that the effects we observe are not due to activation of RhoA, because constitutively active RhoAV14 primarily affects traffic through the basolateral early endosomes, and a central aggregate is not formed (Leung *et al.*, 1999). Through modifications of the lipid bilayer, both phospholipase D and phosphoinositol-4-phosphate 5-OH kinase are known to affect the ability of coat proteins to bind to organellar membranes (Liscovitch and Cantley, 1995; De Camilli *et al.*, 1996; Liscovitch, 1996). Perhaps the coats that specify apical targeting are selectively disrupted in cells expressing Rac1V12. Activation of PI-3-K is especially intriguing because transcytosis of the pIgR is inhibited by wortmannin, a potent inhibitor of PI-3-K (Hansen *et al.*, 1995). Uncontrolled activation of PI-3-K and its effectors may have dramatic effects on postendocytic traffic. The target(s) of Rac1 will have to await additional studies because the signals that specify apical sorting in the endocytic pathway of polarized epithelial cells are largely unknown and the apical sorting/budding machinery is undescribed.

The defects in apical membrane traffic observed in Rac1V12-expressing cells may be relevant to understanding cellular physiology in cancerous cells, in which cellular polarity is highly disorganized (Schoenenberger and Matlin, 1991; Schoenenberger *et al.*, 1991). Rho family members have been implicated in cancer progression, and RhoA and Rac1 are required for Ras-mediated transformation (Qiu *et al.*, 1995a,b; Olson, 1996; Vojtek and Der, 1998). Moreover, all of the more than 20 guanine nucleotide exchange factors for members of the Rho family are potentially oncogenic, and this oncogenicity is apparently the result of their inappropriate activation of Rho family members (Olson, 1996; Van Aelst and D'Souza-Schorey, 1997). Uncontrolled Rac1 activation, therefore, could lead to disruption of apically directed membrane traffic, loss of cell polarity, and, ultimately, cellular dysfunction.

ACKNOWLEDGMENTS

We thank Drs. Cann, Ojakian, Walters, Lindstedt, Rodriguez-Boulan, and Mostov for their kind gifts of antibodies and reagents. This work was supported by grants from the National Institutes of Health to G.A. (RO1DK51970) and W.J.N. (GM35527). L.M.F. is supported by The Stanford Neurosciences Training Grant. The Laboratory of Epithelial Biology is supported in part by an equipment grant from Dialysis Clinic, Inc.

REFERENCES

Adam, T., Giry, M., Boquet, P., and Sansonetti, P. (1996). Rho-dependent membrane folding causes *Shigella* entry into epithelial cells. EMBO J. *15*, 3315–3321.

Adamson, P., Paterson, H.F., and Hall, A. (1992). Intracellular localization of the $p21^{rho}$ proteins. J. Cell Biol. *119*, 617–627.

Annaert, W.G., Becker, B., Kistner, U., Reth, M., and Jahn, R. (1997). Export of cellubrevin from the endoplasmic reticulum is controlled by BAP31. J. Cell Biol. *139*, 1397–1410.

Apodaca, G., Aroeti, B., Tang, K., and Mostov, K.E. (1993). Brefeldin-A inhibits the delivery of the polymeric immunoglobulin receptor to the basolateral surface of MDCK cells. J. Biol. Chem. *268*, 20380–20385.

Apodaca, G., Katz, L.A., and Mostov, K.E. (1994). Receptor-mediated transcytosis of IgA in MDCK cells is via apical recycling endosomes. J. Cell Biol. *125*, 67–86.

Aroeti, B., Kosen, P.A., Kuntz, I.D., Cohen, F.E., and Mostov, K.E. (1993). Mutational and secondary structural analysis of the basolateral sorting signal of the polymeric immunoglobulin receptor. J. Cell Biol. *123*, 1149–1160.

Aroeti, B., and Mostov, K.E. (1994). Polarized sorting of the polymeric immunoglobulin receptor in the exocytotic and endocytotic pathways is controlled by the same amino acids. EMBO J. *13*, 2297–2304.

Bacallao, R., Antony, C., Dotti, C., Karsenti, E., Stelzer, E.H.K., and Simons, K. (1989). The subcellular organization of Madin-Darby canine kidney cells during the formation of a polarized epithelium. J. Cell Biol. *109*, 2817–2832.

Barroso, M., and Sztul, E. (1994). Basolateral to apical transcytosis in polarized cells is indirect and involves BFA and trimeric G protein sensitive passage through the apical endosome. J. Cell Biol. *124*, 83–100.

Barth, A.I., Pollack, A.L., Altschuler, Y., Mostov, K.E., and Nelson, W.J. (1997). NH_2-terminal deletion of beta-catenin results in stable colocalization of mutant beta-catenin with adenomatous polyposis coli protein and altered MDCK cell adhesion. J. Cell Biol. *136*, 693–706.

Breitfeld, P., Casanova, J.E., Harris, J.M., Simister, N.E., and Mostov, K.E. (1989a). Expression and analysis of the polymeric immunoglobulin receptor. Methods Cell Biol. *32*, 329–337.

Breitfeld, P.P., Casanova, J.E., McKinnon, W.C., and Mostov, K.E. (1990). Deletions in the cytoplasmic domain of the polymeric immunoglobulin receptor differentially affect endocytotic rate and postendocytotic traffic. J. Biol. Chem. *265*, 13750–13757.

Breitfeld, P.P., Harris, J.M., and Mostov, K.M. (1989b). Postendocytotic sorting of the ligand for the polymeric immunoglobulin receptor in Madin-Darby canine kidney cells. J. Cell Biol. *109*, 475–486.

Brown, A.M., O'Sullivan, A.J., and Gomperts, B.D. (1998). Induction of exocytosis from permeabilized mast cells by the guanosine triphosphatases Rac and Cdc42. Mol. Biol. Cell *9*, 1053–1063.

Cardone, M.H., Smith, B.L., Song, W., Mochley-Rosen, D., and Mostov, K.E. (1994). Phorbol myristate acetate-mediated stimulation of transcytosis and apical recycling in MDCK cells. J. Cell Biol. *124*, 717–727.

Casanova, J.E., Apodaca, G., and Mostov, K.E. (1991). An autonomous signal for basolateral sorting in the cytoplasmic domain of the polymeric immunoglobulin receptor. Cell *66*, 65–75.

Casanova, J.E., Wang, X., Kumar, R., Bhartur, S.G., Navarre, J., Woodrum, J.E., Altschuler, Y.A., Ray, G.S., and Godenring, J.R. (1999). Association of Rab25 and Rab11a with the apical recycling system of polarized Madin-Darby canine kidney cells. Mol. Biol. Cell *10*, 47–61.

Chen, L.-M., Hobbie, S., and Galán, J.E. (1996). Requirement of CDC42 for *Salmonella*-induced cytoskeletal and nuclear responses. Science *274*, 2115–2118.

Cussac, D., Leblanc, P., L'Heritier, A., Bertoglio, J., Lang, P., Kordon, C., Enjalbert, A., and Saltarelli, D. (1996). Rho proteins are localized with different membrane compartments involved in vesicular trafficking in anterior pituitary cells. Mol. Cell. Endocrinol. *119*, 195–206.

De Camilli, P., Emr, S.D., McPherson, P.S., and Novick, P. (1996). Phosphoinositides as regulators in membrane traffic. Science *271*, 1533–1539.

Drubin, D.G., and Nelson, W.J. (1996). Origins of cell polarity. Cell *84*, 335–344.

Fuller, S.D., and Simons, K. (1986). Transferrin receptor polarity and recycling accuracy in "tight" and "leaky" strains of Madin-Darby canine kidney cells. J. Cell Biol. *103*, 1767–1779.

Green, E.G., Ramm, E., Riley, N.M., Spiro, D.J., Goldenring, J.R., and Wessling-Resnick, M. (1997). Rab11 is associated with transferrin-containing recycling compartments in K562 cells. Biochem. Biophys. Res. Commun. *239*, 612–616.

Grindstaff, K.K., Bacallao, R.L., and Nelson, W.J. (1998a). Apionuclear organization of microtubules does not specify protein delivery from the trans-Golgi network to different membrane domains in polarized epithelial cells. Mol. Biol. Cell *9*, 685–699.

Grindstaff, K.K., Yeaman, C., Anandasabapathy, N., Hsu, S.C., Rodriquez-Boulan, E., Scheller, R.H., and Nelson, W.J. (1998b). Sec6/8 complex is recruited to cell-cell contacts and specifies transport vesicle delivery to the basal-lateral membrane in epithelial cells. Cell *93*, 731–740.

Hall, A. (1998). Rho GTPases and the actin cytoskeleton. Science *279*, 509–514.

Hansen, S.H., and Casanova, J.E. (1994). Gsα stimulates transcytosis and apical secretion in MDCK cells through cAMP and protein kinase A. J. Cell Biol. *126*, 677–688.

Hansen, S.H., Olsson, A., and Casanova, J.E. (1995). Wortmannin, an inhibitor of phosphoinositide 3-kinase, inhibits transcytosis in polarized epithelial cells. J. Biol. Chem. *270*, 28425–28432.

Jou, T.-S., and Nelson, W.J. (1998). Effects of regulated expression of mutant RhoA and Rac1 small GTPases on the development of epithelial (MDCK) cell polarity. J. Cell Biol. *142*, 85–100.

Jou, T.-S., Schneeberger, E.E., and Nelson, W.J. (1998). Structural and functional regulation of tight junctions by RhoA and Rac1 small GTPases. J. Cell Biol. *142*, 101–115.

Kozma, R., Ahmed, S., Best, A., and Lim, L. (1995). The Ras-related protein Cdc42Hs and bradykinin promote formation of peripheral actin microspikes and filopodia in Swiss 3T3 fibroblasts. Mol. Cell. Biol. *15*, 1942–1952.

Kroschewski, R., Hall, A., and Mellman, I. (1999). Cdc42 controls secretory and endocytic transport to the basolateral plasma membrane of MDCK cells. Nat. Cell Biol. *1*, 8–13.

Lamaze, C., Chuang, T.-H., Terlecky, L.J., Bokoch, G.M., and Schmid, S.L. (1996). Regulation of receptor-mediated endocytosis by Rho and Rac. Nature *382*, 177–179.

Leung, S.-M., Rojas, R., Maples, C., Flynn, C., Ruiz, W.G., Jou, T.-S., and Apodaca, G. (1999). Modulation of endocytic traffic in polarized MDCK cells by the small GTPase RhoA. Mol. Biol. Cell *10*, 4369–4384.

Li, G., D'Souza-Schorey, C., Barbieri, M.A., Cooper, J.A., and Stahl, P.D. (1997). Uncoupling of membrane ruffling and pinocytosis during ras signal transduction. J. Biol. Chem. *272*, 10337–10340.

Lindstedt, A.D., and Hauri, H.P. (1993). Giantin, a novel conserved Golgi membrane protein containing a cytoplasmic domain of at least 350 kDa. Mol. Biol. Cell *4*, 679–693.

Liscovitch, M. (1996). Phospholipase D: role in signal transduction and membrane traffic. J. Lipid Mediators Cell Signal. *14*, 215–221.

Liscovitch, M., and Cantley, L.C. (1995). Signal transduction and membrane traffic: the PITP/phosphoinositide connection. Cell *81*, 659–662.

Mackay, D.J.G., and Hall, A. (1998). Rho GTPases. J. Biol. Chem. *273*, 20685–20688.

Mariot, P., O'Sullivan, A.J., Brown, A.M., and Tatham, P.E.R. (1996). Rho guanine nucleotide dissociation inhibitor protein (RhoGDI) inhibits exocytosis in mast cells. EMBO J. *15*, 6476–6482.

Molloy, S.S., Thomas, L., VanSlyke, J.K., Stenberg, P.E., and Thomas, G. (1994). Intracellular trafficking and activation of furin proprotein convertase: localization to the TGN and recycling from the cell surface. EMBO J. *13*, 18–33.

Mostov, K.E., and Cardone, M.H. (1995). Regulation of protein traffic in polarized epithelial cells. BioEssays *17*, 129–138.

Murphy, C., Saffrich, R., Grummt, M., Gournier, H., Rybin, V., Rubino, M., Auvinen, P., Lütcke, A., Parton, R.G., and Zerial, M. (1996). Endosome dynamics regulated by a Rho protein. Nature *384*, 427–432.

Nabi, I.R., Le Bivic, A., Fambrough, D., and Rodriguez-Boulan, E. (1991). An endogenous MDCK lysosomal membrane glycoprotein is targeted basolaterally before delivery to lysosomes. J. Cell Biol. *115*, 1573–1584.

Norman, J.C., Price, L.S., Ridley, A.J., Hall, A., and Koffer, A. (1994). Actin filament organization in activated mast cells is regulated by heterotrimeric and small GTP-binding proteins. J. Cell Biol. *126*, 1005–1015.

Norman, J.C., Price, L.S., Ridley, A.J., and Koffer, A. (1996). The small GTP-binding proteins, Rac and Rho, regulate cytoskeletal organization and exocytosis in mast cells by parallel pathways. Mol. Biol. Cell *7*, 1429–1442.

Odorizzi, G., Pearse, A., Domingo, D., Trowbridge, I.S., and Hopkins, C.R. (1996). Apical and basolateral endosomes of MDCK cells are interconnected and contain a polarized sorting mechanism. J. Cell Biol. *135*, 139–152.

Olson, M.F. (1996). Guanine nucleotide exchange factors for the Rho GTPases: a role in human disease? J. Mol. Med. *74*, 563–571.

O'Sullivan, A.J., Brown, A.M., Freeman, H.N., and Gomperts, B.D. (1996). Purification and identification of FOAD-II, a cytosolic protein that regulates secretion in streptolysin-O permeabilized mast cells, as a rac/rhoGDI complex. Mol. Biol. Cell *7*, 397–408.

Parton, R.G., Prydz, K., Bomsel, M., Simons, K., and Griffiths, G. (1989). Meeting of the apical and basolateral endocytic pathways of the Madin-Darby canine kidney cell in late endosomes. J. Cell Biol. *109*, 3259–3272.

Price, L.S., Norman, J.C., Ridley, A.J., and Koffer, A. (1995). The small GTPases Rac and Rho as regulators of secretion in mast cells. Curr. Biol. *5*, 68–73.

Qiu, R.-G., Chen, J., Kirn, D., McCormick, F., and Symons, M. (1995a). An essential role for Rac in Ras transformation. Nature *374*, 457–459.

Qiu, R.-G., Chen, J., McCormick, F., and Symons, M. (1995b). A role for Rho in Ras transformation. Proc. Natl. Acad. Sci. USA *92*, 11781–11785.

Ren, M., Xu, G., Zeng, J., De Lemos-Chiarandini, C., Adesnik, M., and Sabatini, D.D. (1998). Hydrolysis of GTP on Rab11 is required for direct delivery of transferrin from the pericentriolar recycling compartment to the cell surface but not from sorting endosomes. Proc. Natl. Acad. Sci. USA *95*, 6187–6192.

Ridley, A.J., and Hall, A. (1992). The small GTP-binding protein Rho regulates the assembly of focal adhesions and actin stress fibers in response to growth factors. Cell *70*, 389–399.

Ridley, A.J., Paterson, H.F., Johnston, C.L., Diekmann, D., and Hall, A. (1992). The small GTP-binding protein rac regulates growth factor-induced membrane ruffling. Cell *70*, 401–410.

Schmalzing, G., Richter, H.-P., Hansen, A., Schwarz, W., Just, I., and Aktories, K. (1995). Involvement of the GTP binding protein Rho in constitutive endocytosis in *Xenopus laevis* oocytes. J. Cell Biol. *130*, 1319–1332.

Schoenenberger, C.-A., and Matlin, K.S. (1991). Cell polarity and epithelial oncogenesis. Trends Cell Biol. *1*, 87–92.

Schoenenberger, C.-A., Zuk, A., Kendall, D., and Matlin, K.S. (1991). Multilayering and loss of apical polarity in MDCK cells transformed with viral K-ras. J. Cell Biol. *112*, 873–889.

Sheff, D.R., Daro, E.A., Hull, M., and Mellman, I. (1999). The receptor recycling pathway contains two distinct populations of early endosomes with different sorting functions. J. Cell Biol. *145*, 123–139.

Ullrich, O., Reinsch, S., Urbe, S., Zerial, M., and Parton, R.G. (1996). Rab11 regulates recycling through the pericentriolar recycling endosome. J. Cell Biol. *135*, 913–924.

Urbé, S., Huber, L.A., Zerial, M., Tooze, S.A., and Parton, R.G. (1993). Rab11, a small GTPase associated with both constitutive and regulated secretory pathways in PC12 cells. FEBS Lett. *334*, 175–182.

Van Aelst, L., and D'Souza-Schorey, C. (1997). Rho GTPases and signaling networks. Genes Dev. *11*, 2295–2322.

Vojtek, A.B., and Cooper, J.A. (1995). Rho family members: activators of MAP kinase cascades. Cell *82*, 527–529.

Vojtek, A.B., and Der, C.J. (1998). Increasing complexity of the ras signaling pathway. J. Biol. Chem. *273*, 19925–19928.

Watarai, M., Kamata, Y., Kozaki, S., and Sasakawa, C. (1997). Rho, a small GTP-binding protein, is essential for *Shigella* invasion of epithelial cells. J. Exp. Med. *185*, 281–292.